



UNIVERSITAT POLITÈCNICA
DE CATALUNYA
BARCELONATECH



MASTER THESIS

Digital Adaptive Predistortion for Unmanned Aerial Vehicle Communications with Under Sampling Method

Teng Wang

SUPERVISED BY

Pere Lluís Gilabert

Universitat Politècnica de Catalunya
Master in Aerospace Science & Technology
December 2014

This Page Intentionally Left Blank

Digital Adaptive Predistortion for Unmanned Aerial Vehicle Communications with Under-Sampling Method

BY
Teng Wang

DIPLOMA THESIS FOR DEGREE
Master in Aerospace Science and Technology

AT
Universitat Politècnica de Catalunya

SUPERVISED BY:
Pere Lluís Gilabert
Department of Signal Theory and Communications

This Page Intentionally Left Blank

ABSTRACT

Nowadays, the Unmanned Aerial Vehicle (UAV) become more and more popular in aerial photography, especially in mini and micro size UAV. The UAV used for aerial photography usually use a high power video transfer communication block to send the real time video signal to the ground station, which is high power consuming. It is important to increase the power efficiency of on-board communication system for improving the endurance of small-scale UAVs.

The power amplifier (PA) is the most power consuming component among all the units in communication system. Given the nature feature of the PA, it tends to be either linear response or higher power efficiency, but rarely both. The PA with high power efficiency always has a horrible non-linear distortion performance that discards its use.

There are several available linearization methods to compensate the non-linear behavior of PA. Among them the digital predistortion (DPD) method is widely used with the development of digital electronic technology. However, the design cost of DPD block itself should be taken into consideration. The DPD linearizer requires a feedback path to monitor the PA behavior and the analog to digital convertor (ADC) is a critical component from the cost and efficiency point of view. The price of ADC makes a prominently contribution to the total cost of DPD linearizer.

The price of the ADC is usually proportional to the sampling frequency, which, according to the Nyquist-Shannon sampling theorem, should be higher than twice the bandwidth of the communication's signal. In this thesis, we will present an under sampling method and its supporting algorithm aimed to decrease the frequency rate requirements of the ADC to perform the DPD linearization. In this way, ADC with lower sampling frequency is able to be used in the DPD feedback loop and thus decrease the total cost without compromising the linearization performance. The theoretical analysis will be first presented in this thesis and then experimental results showing the performance of the DPD with under-sampling method will be shown and discussed.

This Page Intentionally Left Blank

Table of Contents

INTRODUCTION	1
CHAPTER 1 PROBLEM STATEMENT.....	4
1.1. Statement of UAV Communication System	4
1.2. The Battery Limitation	5
1.3. PA Linearity vs Efficiency.....	6
1.4. Non-linear Behavior of PA	8
1.5. Memory Effects of PA.....	10
1.6. PA Linearization Methods.....	12
CHAPTER 2 THE PRINCIPLE OF DIGITAL PREDISTORTION	14
2.1. PA Modulation.....	14
2.2. DPD Implementation.....	16
2.2.1. Direct Learning Method	17
2.2.2. Indirect Learning Method	18
2.3. The Feedback Path and the Importance of the Analog-to-Digital Converter (ADC)	20
CHAPTER 3 DESCRIPTION OF THE UNDER SAMPLING THEORY	22
3.1. Definition of Under Sampling	22
3.2. DPD coefficients calculation	22
3.3. The Statistical Sampling of the Linear Regression Model	24
3.4. The Problem of Aliasing.....	27
3.5. Upper Limitation of the Under Sampling Ratio.....	29
CHAPTER 4 ALIGNING PROBLEM.....	31
4.1. Problem Statement	31
4.2. Linearity Dependence Algorithm (LDA)	32
4.3. The Problem of Stability.....	34
CHAPTER 5 EXPERIMENTAL PERFORMANCE	35
5.1. Statement of Test Environment	35
5.1.1. Test Signal.....	35
5.1.2. Analog Amplifying Part	36
5.1.3. Feedback Path.....	37
5.1.4. Matlab Program and PA Model	37
5.2. LDA Instability Evaluation	39
5.3. Experimental Result of US-DPD.....	40
CHAPTER 6 CONCLUSIONS.....	43

This Page Intentionally Left Blank

List of Figures

Figure 1.1 Common Video Transfer Block on Market	4
Figure 1.2 The Behavior of Ideal and Real PA.....	7
Figure 1.3 Fixes and Dynamic Power Supply [6]	7
Figure 1.4 Diagram of Dynamic Supply Implementation in DPD	8
Figure 1.5 Output Signal in Frequency Domain of Non-linear PA with Bandwidth Input Signal	10
Figure 1.6 AM-AM Characteristic of Real PA Behavior	11
Figure 1.7 Principle of Predistortion [4].....	13
Figure 1.8 The Performance of DPD Linearization	13
Figure 2.1 The Matrix Formation of PA Model	16
Figure 2.2 The DPD Implementation in Mathematical view.....	17
Figure 2.3 Indirect Learning Method	17
Figure 2.4 Indirect Learning Method	19
Figure 3.1 The Matrix of Memory Polynomial Model.....	23
Figure 3.2 Matrix Division of the RLS Algorithm.....	23
Figure 3.3 An Example of Linear Equation	25
Figure 3.4 Average PPMC Value of Nearby Equations with a Given Gap.....	26
Figure 3.5 The Extraction of Equations in US-DPD	27
Figure 3.6 Effects of Aliasing when Sampling a Signal [1]	28
Figure 3.7 The Comparing of Full Rate Sampling and Under Sampling ADC-DAC Loop	28
Figure 4.1 The Result of Cross-Correlation in Under Sampling Situation.....	32
Figure 4.2 Linearity Dependence of Original Signal and Down Sampled Signal	33
Figure 4.3 LDA Detection Result When Change USR	33
Figure 4.4 Linearity Dependence Value with different Delay Assumption	34
Figure 5.1 The Spectra of LTE Signal.....	36
Figure 5.2 The Schematic of Experimentation Set-up.....	37
Figure 5.3 The Diagram of Matlab Program.....	38
Figure 5.4 NMSE and ACLR Values When Misalignment Happens on DPD	39
Figure 5.5 The DPD performance in ACLR with Forced Delay and LDA Restoration.....	40
Figure 5.6 Iteration numbers in Different USR and Different DPD Threshold, Static Supply	41
Figure 5.7 Iteration Numbers in Different USR and Different DPD Threshold, Dynamic Supply	41
Figure 5.8 DPD Performance in Different USR	42
Figure 6.1 Entirety Time of DPD Updating with USR	43

This Page Intentionally Left Blank

List of tables

Table 2-1 The DPD Performance in Different Parameters20

Table 2-2 The Price of ADC with Different Frequency [15]21

Table 5-1 DPD Performance Evaluated by NMSE in Different USR42

This Page Intentionally Left Blank

INTRODUCTION

Nowadays, the Unmanned Aerial Vehicle (UAV) become more and more popular in aerial photography, especially in mini and micro size UAV. Small-scale UAVs are usually supported by small size lithium polymer batteries. Given the unsatisfactory performance of recent battery technic, most small-scale UAVs confront with the problem of insufficient on board energy. Addition to receive the control signal, the UAV used for aerial photography usually use a high power video transfer communication block to send the real time video signal to the ground state, which is high power consuming. Contrast to the power consuming of propulsion system which is proportional to the mass quantity, the power requirement for sending the single to ground station is proportional to the distance between UAV and the ground station. In this way, small-scale UAVs which works in long distance faces the worst situation because they their on-board batteries are much smaller than large-scale UAVs but consuming as much power as the latter one for video transferring. Due to the low selling price and operation cost of small-scale UAVs, it is important to increase the power efficiency of on-board communication system for improving the endurance of small-scale UAVs.

The power amplifier (PA) is the most power consuming component among all the units in communication system. Given the nature feature of PA, it tends to be either linear response or higher power efficiency, but rarely both. The linear PA (class A, class AB) is able to transfer the RF signal properly but the typical efficiency around 10% when considering amplitude and phase modulated signals with high peak-to-average power ratio (PAPR). In contrast, high efficiency PA (class E, F) offers over 70% power efficiency but has a horrible non-linear distortion performance that discards its use.

There are several available linearization methods to compensate the non-linear behavior of PA. Among them the digital predistortion (DPD) method is widely used with the development of digital electronic technology. However, the design cost of DPD block itself should be taken into consideration, especially when applied on low cost small-scale UAV. The DPD linearizer requires a feedback path to monitor the PA behavior. Thus, besides the digital signal processing elements in the forward path, the analog to digital convertor (ADC), necessary to digitize the baseband equivalent PA output signal, is a critical component from the cost and efficiency point of view. The price of ADC makes a prominently contribution to the total cost of DPD linearizer.

The price of the ADC is usually proportional to the sampling frequency, which, according to the Nyquist-Shannon sampling theorem, should be higher than twice the bandwidth of the communication's signal. In this thesis, we will present an under sampling method and its supporting algorithm aimed to decrease the frequency rate requirements of the ADC to perform the DPD linearization. In this way, ADC with lower sampling frequency is able to be used in the DPD feedback loop and thus decrease the total cost without compromising the linearization performance. The theoretical analysis will be first presented in this thesis and then experimental results showing the performance of the DPD with under-sampling method will be shown and discussed.

Therefore, this thesis is organized as follows:

Chapter I introduces the problem of the UAV on-board communication system. The non-linear behavior and memory effect of the PA will be described.

Chapter II describes the principles of the under-sampling algorithm. It addresses the definition of under sampling method and why it does not affect the sampling accuracy in the DPD identification.

Chapter III describes the solution of aliasing problem when applying under sampling method. Both theoretical analysis and test results of the novel linearity dependence alignment (LDA) is stated to validate its feasibility.

Chapter IV addresses the implementation of under sampling DPD. The recursive least squares (RLS) is also addressed as a cooperative identification method with the under sampling technique. The test result will show the feasibility of under sampling DPD and the benefit of co-working with RLS.

Chapter V shows the perspective of using narrow bandwidth ADC to further decreasing the total cost of communication system.

Finally, in Chapter VI the main conclusions of the under sampling DPD with RLS method will be given.

This Page Intentionally Left Blank

Chapter 1

Problem Statement

1.1. Statement of UAV Communication System

The small-scale UAVs are widely used in aerial photography. With the developing of autopilot, and radio control technic, small-scale UAVs are allow to operate in a radius of 10-30 kilometer which is far beyond line of sight. In this usage, the UAV needs to send real time video back to the ground station for the photographer. In this way the quantity and timeliness of the video transfer is highly required in case to take good and correct photo for target positions of objects. For sending the real time video to ground station, the video will be firstly obtained by the camera and processed by on-board computer into digital signal. The signal will then be modulated and converted to analog signal. The analog signal will be enlarged by power amplifier (PA) of the communication system in case to be propagated by antenna. The integrated block form video signal processing to the antenna is usually called video transfer block (VTB), as in Figure 1.1.



Figure 1.1 Common Video Transfer Block on Market

The VTB that available on the market mostly works with 2.4GHz and 5.8GHz carrier frequency and 10 MHz to 20 MHz bandwidth of long term evolution (LTE) signal [1] [2]. There are also several different channels of each carrier signal. For example the 2.4 GHz video transfer usually have 20-40 different channels [3], the transmitter and receiver is able to detect the available and occupied channel in their working space to avoid interaction. This is based on a strict principle that every VTB should only send their own channel without leaking significant noise to other adjacent channels. An indicator called Adjacent Channel Leakage Ratio (ACLR) is used as the evaluation standard. The definition of ACLR is as following:

$$\text{ACLR} = 10 \log \left(\frac{\int_{f_{adj}} |Y_{out}[f]|^2 df}{\int_{f_{chan}} |Y_{out}[f]|^2 df} \right) \quad (1-1)$$

Where the Y_{out} is the Fourier transform of PA output signal.

In addition, the quality of the video is also higher required as the photographer is not able to work with unacceptable noise on the screen. An indicator called Normalized Mean Square Error (NMSE) is used to evaluate the quality of transferred video signal. The definition of NMSE at the PA output is as follows:

$$\text{NMSE} = 10 \log \left(\frac{\sum_{n=1}^L |y_{out}[n] - x_{in}[n]|^2}{\sum_{n=1}^L |x_{in}[n]|^2} \right) \quad (1-2)$$

Where the y_{out} is the output of PA and x_{in} is the input signal.

1.2. The Battery Limitation

Although small scale UAVs have significant advantage in selling price and operational cost that allows most individuals and small companies are afford to purchase, the drawback of insufficient electronic power is also leaded by the body size. As the capacity of the battery is proportional with the weight of the battery thus also is proportional with the total weight of UAV itself.

There are two main part of power consuming of the UAV. For UAVs lighter than 100kg, no matter the fixed wing, multi-rotor or the helicopter, the aerodynamics performance does not change obviously with size. Thus the lift-drag ratio (for the vertical aircraft is the lift efficiency) will remain the same. As the propulsion force requirement is proportional to the lift-drag ratio and take-off weight. So, for small size UAVs, the propulsion requirement is only proportional with its weight. In this way, the small size UAV with lighter battery also need less propulsion power. The endurance is not significantly influenced by the size in the view of propulsion.

On the other hand, the power requirement of the communication system (i.e. mainly the video transfer part), is directly related with the maximum allowed distance between UAV and ground station. UAVs operating in the same distance need support the communication system with same level of electronics, no matter what size they are. As a result, the small size UAV has significant lower endurance than large-scale ones, but the endurance performance is also improvable by reducing the power cost of communication system.

In order to determine the efficiency of power amplifier quantitatively, a critical indicator called Power Added Efficiency is defined as following:

$$\mathbf{PAE} = \frac{P_{out} - P_{in}}{P_{DC}} \quad (1-3)$$

Where P_{out} is the power of PA is output signal, P_{in} is the power of PA input signal and P_{DC} is the power that consumed by PA.

For long rang operating UAV, due to the delay of telecommunication, it is not possible to control by pilot on the ground. Instead the autopilot is applied for UAV control. In this way, the major part among the communication system is VTB. Comparing with other units in TVB, the power amplifier (PA) is the most consuming electronic component. Given the nature feature of PA, it tends to be either linear responding or high efficiency, but not both. The common linear PA used in VTB has a poor efficiency around 10% which is nearly unable to use in long distance situation. In a usual case, a UAV operating in not really clear electromagnetic environment and about 16 km away from ground station needs 200 W of output power to send the video to ground station [2]. As the efficiency is around 10% PAE, the power of TVB on that UAV will reach approximately 2 KW, which is unacceptable for size UAV with only 20Ah-22V battery capacity. High efficient PAs, such as the switched-mode PAs (class-E, class-F), present a terrible non-linear behavior that will deteriorate the quality of video and leak a lot noise to adjacent channels. The details of the nonlinear PA behavior will be described in following subsections.

1.3. PA Linearity vs Efficiency

Before presenting the behavior of PA, a critical indicator called Pear-to-Average Power Ratio is defined as following:

$$\mathbf{PAPR} = 10 \log_{10} \left(\frac{P_{Peak}}{P_{Average}} \right) \quad (1-4)$$

Where P_{Peak} is the power of the signal maximum and $P_{Average}$ is the average power of the signal. Common values of PAPR are 0 dB for a single-tone, 1.5 dB for a GSM signal [4], between 12.8 and 14.8 dB for a LTE signal [5].

The ideal PA is usually regarded as a pure proportional function with a power limitation, as depicted in left side of Figure 1.2. This PA responding graph describes the relation between the amplitude of input and output signal, which is also called AM-AM characteristic. The output signal will be amplified with a given gain if the input value is lower than the limitation. But in real case, the PA responding is a curve with only a small part of linear response. When the value of input signal is inside this range, the PA output will be almost linear. If the input signal is beyond the linear range, the output will not be proportional to the input signal anymore, which is called the non-linear behavior. The detail of non-linear behavior will be presented in the following section. If

we want the PA working in the linear part, the maximum value of the input signal should be smaller than the limitation of linear range. In this way the actual input range of PA should be larger than the required amplification. Thus the power consumption is also increased, which reduces the power efficiency of PA.

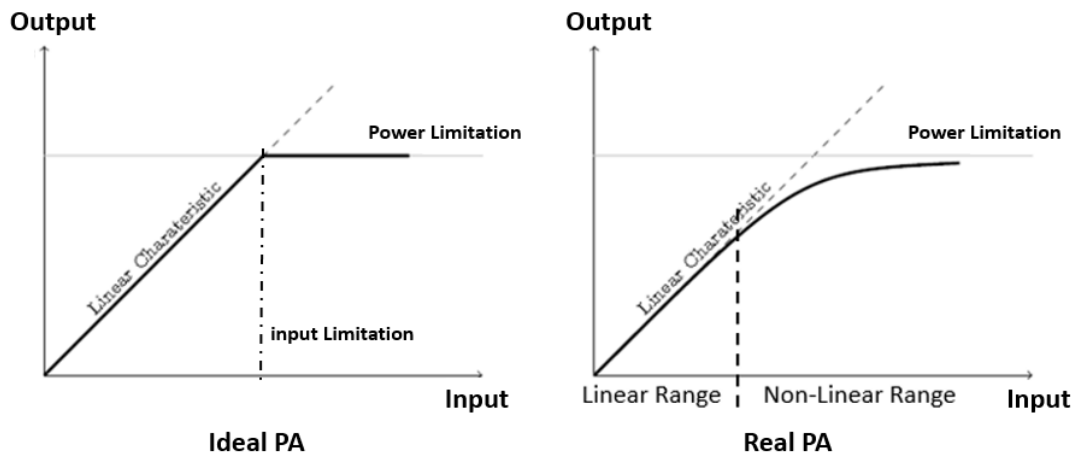


Figure 1.2 The Behavior of Ideal and Real PA

The power consumption of PA is not related to the input signal but to the voltage of the power supply. However, the voltage requirement of PA supply is proportional to the PA's input signal. Thus, if the supply power is fixed, it should be higher enough to support the peak value of the input signal. As a result, when the input signal is lower than the peak level, the excess power supplied to the PA will be dissipated as heat. As shown in Figure 1.3, as the PAPR of LTE signal is high, the power dissipated as heat will also be huge

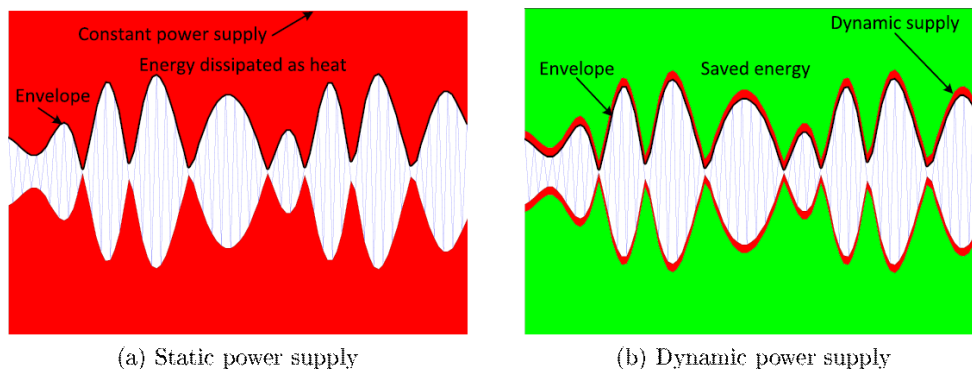


Figure 1.3 Fixes and Dynamic Power Supply [6]

A suitable solution to overcome this problem is to use an amplifier whose voltage supply is dynamically adjusted depending on the required output voltage [7]. This

approach is known as Dynamic Supply. As depicted in Figure 1.4, most of the energy wasted as heat before is saved while implementing dynamic supply and it will increase the total efficiency of the radio transmitter in about 20 %-30 % [8].

In case to apply the dynamic supply to PA, the envelope of the input signal will first be generated and then amplified as the power supply of PA. As depicted in Figure 1.6, the Envelope Generator generates the envelope $E_s[n]$ of input signal $u[n]$ and then the envelop amplifier (EA) will amplify the envelope as the power supply of PA.

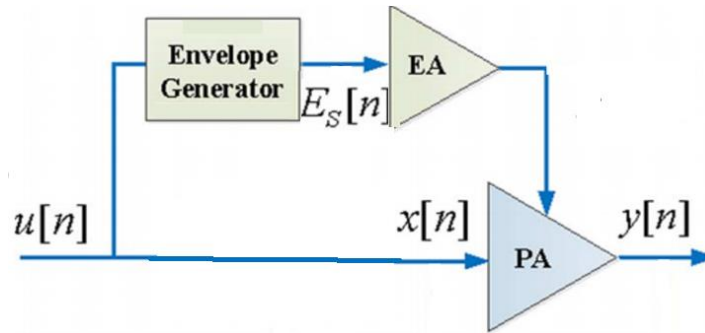


Figure 1.4 Diagram of Dynamic Supply Implementation in DPD

1.4. Non-linear Behavior of PA

The non-linear character of PA is usually describes as the polymer function between the input and output [9], which is defined as following:

$$\hat{y}[n] \cong \sum_{p=0}^P \gamma_p \cdot x[n] \cdot |x[n]|^p \quad (1-5)$$

Where $\hat{y}[n]$ is the estimation value of PA output, $x[n]$ is the input value and γ_p are the coefficients of the function. For simplicity, let the function of PA be the three order polymer function which is defined as:

$$\hat{y}[n] \cong a_1 \cdot x[n] + a_2 \cdot x[n]^2 + a_3 \cdot x[n]^3 \quad (1-6)$$

When the input signal is signal tone signal, which is defined as:

$$x(t) = A \cdot \cos(\omega t) \quad (1-7)$$

The PA output will be as following:

$$y(t) = \frac{1}{2}(a_2 A^2) + \left(a_1 A + \frac{3}{4} a_3 A^3\right) \cdot \cos(\omega t) + \frac{1}{2}(a_2 A^2) \cdot \cos(2\omega t) + \frac{1}{4}(a_3 A^3) \cdot \cos(3\omega t) \quad (1-8)$$

In addition to the tone with original signal frequency ω , the output signal includes several tones with different frequency. Those tones are created by the non-linear behavior of PA, which are called distortion. The non-linear distortion are classified by their frequencies, which showed as following:

The **DC component**, which has the frequency of zero.

In this case is: $\frac{1}{2}(a_2A^2)$;

The **Harmonic distortion**, which has the frequency of multiple of original signal.

In this case are: $\frac{1}{2}(a_2A^2) \cdot \cos(2\omega t) + \frac{1}{4}(a_3A^3) \cdot \cos(3\omega t)$

The Harmonic distortion also can be subdivided into several kinds by the multiple, like:

2nd order Harmonic distortion which has frequency of 2ω

3rd order Harmonic distortion which has frequency of 3ω

When the input signal is not a signal tone, the intermodulation distortion happens. For simplicity, let the input signal is a dual-tone signal for example:

$$x(t) = A_1 \cdot \cos(\omega_1 t) + A_2 \cdot \cos(\omega_2 t) \quad (1-9)$$

In this case the output signal will be:

$$\begin{aligned} y(t) = & \alpha_0 \\ & + \alpha_{1,1} \cos(\omega_1 t) + \alpha_{1,2} \cos(\omega_2 t) \\ & + \alpha_{2,1} \cos(2\omega_1 t) + \alpha_{2,2} \cos(2\omega_2 t) \\ & + \alpha_{3,1} \cos(3\omega_1 t) + \alpha_{3,2} \cos(3\omega_2 t) \\ & + \alpha_4 (\cos((\omega_1 + \omega_2)t) + \cos((\omega_1 - \omega_2)t)) \\ & + \alpha_5 (\cos((2\omega_1 + \omega_2)t) + \cos((2\omega_1 - \omega_2)t)) \\ & + \alpha_4 (\cos((\omega_1 + 2\omega_2)t) + \cos((\omega_1 - 2\omega_2)t)) \end{aligned} \quad (1-10)$$

As shown in equation 1-10, when the input signal has not only one frequency, the output signal contains a new kind of created signal with the mixed frequency. This kind of non-linear distortion is defined as:

The **Intermodulation distortion** (IMD), which has the frequency of a linear combination of input frequency. This distortion is also divided by the number of combination:

2nd order Intermodulation distortion

In this case is: $\alpha_4 (\cos((\omega_1 + \omega_2)t) + \cos((\omega_1 - \omega_2)t))$

3rd order Intermodulation distortion

$$\begin{aligned} \text{In this case are: } & +\alpha_5(\cos((2\omega_1 + \omega_2)t) + \cos((2\omega_1 - \omega_2)t)) \\ & +\alpha_4(\cos((\omega_1 + 2\omega_2)t) + \cos((\omega_1 - 2\omega_2)t)) \end{aligned}$$

When the input signal has a continue bandwidth instead of individual tones, like most actual communication signal, the non-linear behavior become very complex that is very difficult to describe in analysis equations. The appearance in frequency domain the expansion of bandwidth, as drawn in Figure 1.5

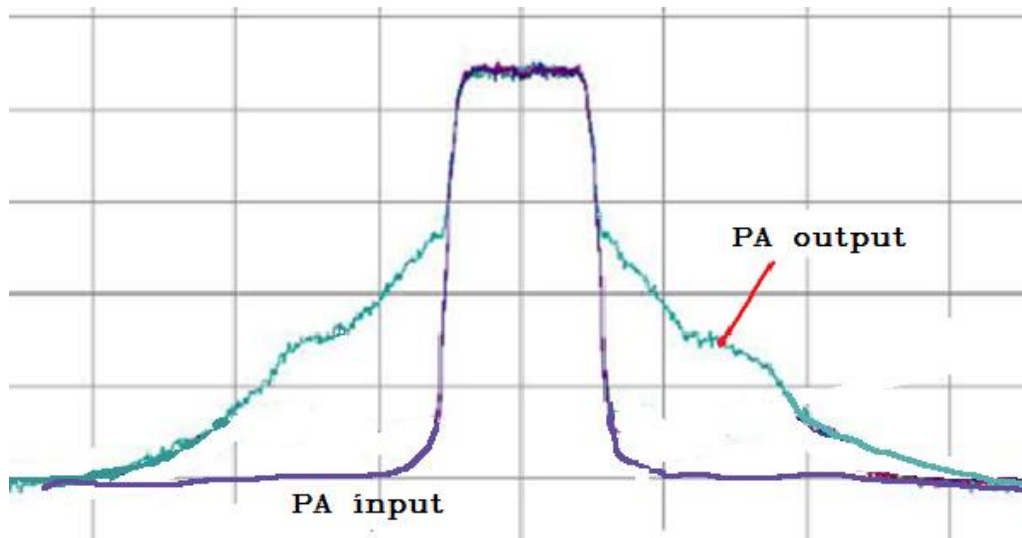


Figure 1.5 Output Signal in Frequency Domain of Non-linear PA with Bandwidth Input Signal

This phenomenon is called the **spectral regrowth**. It is mainly due to the IMD of PA non-linear behavior. It leaks a lot of noise in to the adjacent channels that deteriorate the communication quality of the whole frequency area. Thus the non-linear PA is not allowed to use directly in communication according to the regulation. The spectral regrowth is usually obvious in a range that five times the bandwidth of input signal [10]. The ACLR metric is used to quantify the severity of the spectral regrowth.

1.5. Memory Effects of PA

In addition to the non-linear behavior of PA, the AM-AM characteristic graph of PA is commonly observed as a multi-value function instead of signal value function, as depicted in Figure 1.6.

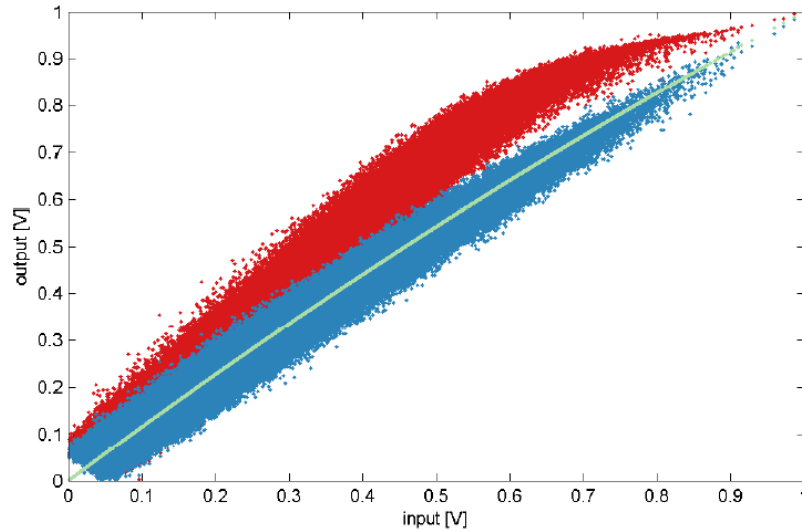


Figure 1.6 AM-AM Characteristic of Real PA Behavior

Clearly, the PA will always have a signal output value, i.e. the voltage, due to its physical foundation. This “multi-value function” phenomenon is officially called the memory effect which mainly leads by the bias circuitry and self-heating [11]. In practical, memory behavior is usually described by multi-input function, i.e. the output of PA is not only related with the input at the same moment, but also influenced by old signals that just been amplified by the PA. The new PA responding function with memory effects is defined as:

$$\hat{y}[n] \cong \sum_{n=0}^N f_n(x[n - \tau_n]) \tag{1-11}$$

Where f_n is a signal value mapping between the input and output signal and τ_n is the delay sequence of input signal.

In this way, the AM-AM graph is not the accurate function graph of the PA input and output but an approximate description. The reason that the output is variable for a given input value is this input value is the mainly but not the only argument of PA responding function and the other argument, i.e. the historical signals are also the arguments of PA responding function.

A further result is given by Kim and Konstantinou is the general combination of the non-linear behavior and the memory effect, which is called Memory Polynomial model. It is defined as following:

$$\hat{y}[n] = \sum_{i=0}^N \sum_{p=0}^P a_{pi} \cdot x[n - \tau_i] \cdot |x[n - \tau_i]|^p \tag{1-12}$$

Where $x[n - \tau_i]$ is the input signal, τ_i the sequence of delay selection, N is the number of delays, P is the number of order and γ_{pi} is the DPD coefficient.

The Memory Polynomial model plays an important role in the field of PA modulation and helps to develop the linearization method for non-linear PA, which will be discussed in next subsection.

1.6. PA Linearization Methods

In addition to the non-linear behavior of PA, the AM-AM graph of PA is commonly observed as a multi-value function instead of signal value function, as depicted in Figure 1.7.

Given the high power efficiency performance of non-linear PA, it is attractive to develop linearization methods. Once the non-linear PA is linearized and able to apply, it will significantly decrease the power consumption of the communication system as discussed before. Several linearization methods are available in engineering implementation. Digital predistortion method are growing rapidly with the developing of microelectronics technology, especially the digital signal processing hardware like Digital Signal Processor (DSP) and Field Programmable Gate Array (FPGA).

Feedback techniques

Feedback is one of the classic control techniques in which the output of the signal is used to change parameters at the input in order to achieve the required goal. It is simple to implementation but not stable when facing the wide band signals.

Feedforward techniques

The basis for feedforward techniques is quite simple: the output of the signal is reduced to the same level of the input and a subtraction is performed in order to keep the distortion. It is sensitive with the system delay detection.

Predistortion techniques

Digital Predistortion (DPD) linearization is one of the most suitable techniques to compensate for the nonlinear behavior of PAs and deal with the trade-off between power efficiency and quality of the transmitted signal. As shown in Figure 1.7, the principle of predistortion is to change the signal before it goes into PA based on the behavior of PA. Once the input and output signal of PA is captured, the non-linear behavior of PA will be modeled. This model will help the DPD to distort the signal in advance to counteract the PA's distortion. In this way, those two part of distortion will cancel each other and the output of PA will become linear. Figure 1.8 depicts the PA performance with and without DPD of a 2 GHz frequency and 20 MHz bandwidth LTE signal. On the left is the spectral regrowth behavior of PA output signal and on the right is the AM-AM characteristic before and after DPD compensation. It is obvious that DPD compensates for the non-linear behavior of the PA and reduces the spectral regrowth.

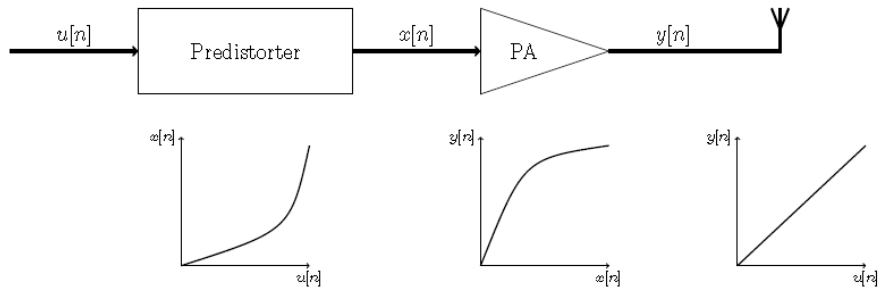


Figure 1.7 Principle of Predistortion [4]

The next chapter will present a more in-depth description of the principles of DPD linearization.

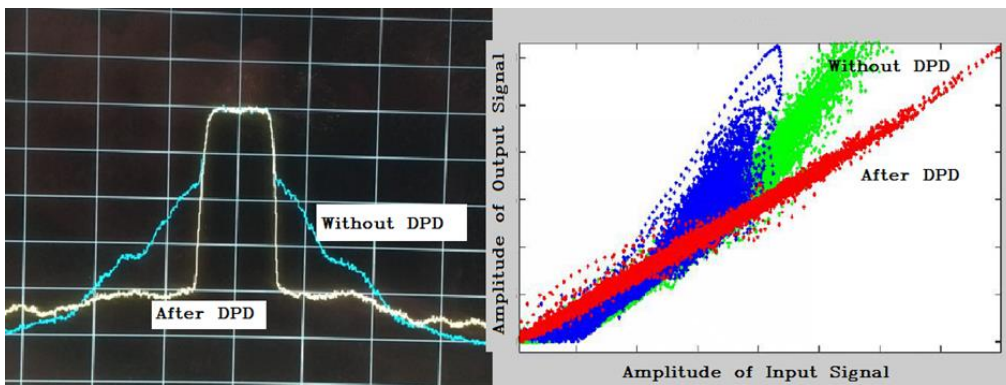


Figure 1.8 The Performance of DPD Linearization

Chapter 2

The Principle of Digital Predistortion

The core idea of predistortion linearization is using a nonlinear function to change the signal before it goes into the PA. Then, this pre-modified signal will be affected by the non-linear behavior of PA. Finally, at the PA output, the resulting signal will present a linear characteristic with respect to the original one. The function used to change the original signal is based on the non-linear characteristic of the PA. In addition, the behavior of PA may be time-variant due to thermal variations or the statistics of the input signal. Thus, adaptive identification methods are widely applied to support digital predistortion.

2.1. PA Modulation

As mentioned in section 1.6, modeling the PA behavior is the first step for implementing DPD. The undetermined coefficient method is the usual way to model the PA, i.e. choosing a model that can describes the behavior of PA in a general way and then using the input and output signals to calculate the coefficients of the model. Modeling the PA nonlinear behavior has been widely studied and there are many technical papers in literature addressing this topic. The most popular and fundamental model is the Memory Polynomial model which was mentioned in section 1.5. It directly reveals the basic phenomenon of PA and is able to characterize the behavior of most of the power amplifiers. In this thesis, Memory Polynomial model will also be chosen to apply in DPD linearization.

The expression of Memory Polynomial model is defined as:

$$\hat{y}[n] = \sum_{i=0}^N \sum_{p=0}^P a_{pi} x[n - \tau_i] \cdot |x[n - \tau_i]|^p \quad (2-1)$$

where $\hat{y}[n]$ is the estimation value of the PA output, $x[n]$ is the input value and $a_{i,j}$ are the coefficients of the function. For a sequence of input samples, n is the serial number of the samples in the sequence. The τ_i is the *memory taps* sequence. It could be either consecutive or non-consecutive.

For simplicity, a Memory Polynomial model with nonlinear order 2 and memory depth 1 is used in the following to introduce the method of PA modeling,

$$\begin{aligned} \hat{y}[n] \cong & a_{1,0} \cdot x[n - \tau_1] + a_{2,0} \cdot x[n - \tau_1] \cdot |x[n - \tau_1]|^1 + a_{3,0} \cdot x[n - \tau_1] \cdot |x[n - \tau_1]|^2 \\ & + a_{1,1} \cdot x[n - \tau_2] + a_{2,1} \cdot x[n - \tau_2] \cdot |x[n - \tau_2]|^1 + a_{3,1} \cdot x[n - \tau_2] \cdot |x[n - \tau_2]|^2 \end{aligned} \quad (2-2)$$

It was proved by Ahmed et al. [12] that a non-uniform distribution of memory taps leads to a better performance of DPD. Additionally, τ_1 usually corresponds to the non-delayed contribution of the input, i.e. τ_1 equals to 1. For simplicity, in this example the memory taps defined as

$$\tau = [0, 1] \quad (2-3)$$

The number of the equations is usually the same as the number of samples in the sequence, which is called the DPD model equations. To save the length when the order and memory depth is large, the $x[n - \tau_i] \cdot |x[n - \tau_i]|^{j-1}$ in equations is also written as x_{n-i}^j , where j is the exponent and i is the delay. These equations are usually written using the vector formation as:

$$[x_n, x_n^2, x_n^3, x_{n-1}, x_{n-1}^2, x_{n-1}^3] \cdot [a_{1,0}, a_{2,0}, a_{3,0}, a_{1,1}, a_{2,1}, a_{3,1}]^T = [\hat{y}_n] \quad (2-4)$$

Where $[]^T$ means the transpose of the matrix and n is the number of the sample in the digital signal sequence.

For simplicity, equation 2-5 is also written as:

$$\mathbf{x}(n) \cdot \mathbf{a}(n)^T = \hat{\mathbf{y}}[n] \quad (2-5)$$

$$\text{Where } \mathbf{x}(n) = [x_n, x_n^2, x_n^3, x_{n-1}, x_{n-1}^2, x_{n-1}^3]$$

$$\mathbf{a}(n) = [a_{1,0}, a_{2,0}, a_{3,0}, a_{1,1}, a_{2,1}, a_{3,1}]$$

Let us now consider that the input sequence $x[n]$ has 100 samples, from $x[1]$ to $x[100]$, and the value of $x[0]$ is also available in case to calculate the memory depth item of $x[1]$. The number of equations will also be 100. The matrix formation is applied to arrange there equations in a clear way, which is called as DPD model matrix. It is shown in Figure 2.1.

$$\begin{array}{ccc}
 \mathbf{X} & \mathbf{w} & \mathbf{y} \\
 \left[\begin{array}{c} x_1, x_1^2, x_1^3, x_0, x_0^2, x_0^3 \\ x_2, x_2^2, x_2^3, x_1, x_1^2, x_1^3 \\ x_3, x_3^2, x_3^3, x_2, x_2^2, x_2^3 \\ \vdots \\ x_{100}, x_{100}^2, x_{100}^3, x_{99}, x_{99}^2, x_{99}^3 \end{array} \right] & \left[\begin{array}{c} a_{1,0} \\ a_{2,0} \\ a_{3,0} \\ a_{1,1} \\ a_{2,1} \\ a_{3,1} \end{array} \right] & = \left[\begin{array}{c} \hat{y}_1 \\ \hat{y}_2 \\ \hat{y}_3 \\ \vdots \\ \hat{y}_{100} \end{array} \right]
 \end{array}$$

Figure 2.1 The Matrix Formation of PA Model

For convenience, we now use the matrix formulation where \mathbf{X} , \mathbf{w} , and \mathbf{y} are the data matrix model, the vector of coefficients and the estimated PA output vector, respectively. Using the matrix formulation, it results:

$$\mathbf{X} \cdot \mathbf{w} = \mathbf{y} \quad (2-6)$$

The detail of solving the \mathbf{w} will be discussed later.

2.2. DPD Implementation

As discussed before, we can obtain a PA behavioral model from input and output observations. Moreover, this behavioral model can be later used to calculate the digital predistorter linearizer. In mathematical view, when the coefficient of the model is acquired, it is able to implement it in DPD by calculating the inverse function of PA model, as shown in the following:

However, the open loop implementation shown in the Figure is only suitable for narrow band of operating conditions [14]. So it is necessary to make the predistortion adaptive in order to extend this band of operating conditions in which the coefficients are adequate. Under this situation, the coefficient of the inverse function are not easy to update unless the whole parameters are recalculated. Thus, the DPD method should be implemented in another way that is able to support the adaptive algorithm and also has low computational complexity.

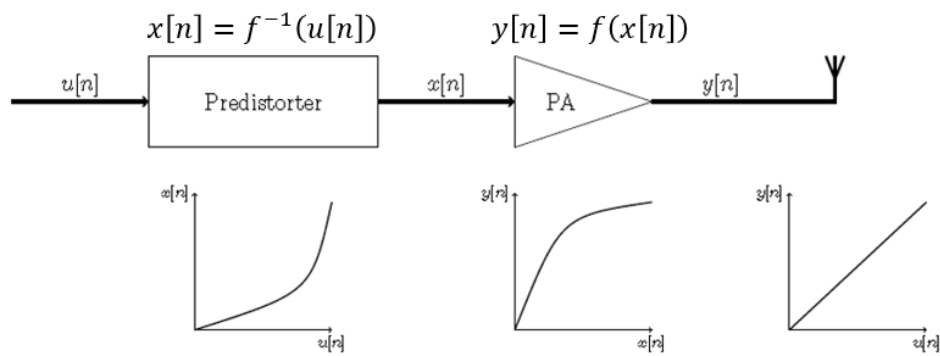


Figure 2.2 The DPD Implementation in Mathematical view

Two major adaptive identification methods are commonly used in DPD implementation.

2.2.1. Direct Learning Method

The block diagram of the DPD extraction based in the direct learning method is shown in Figure 2.3.

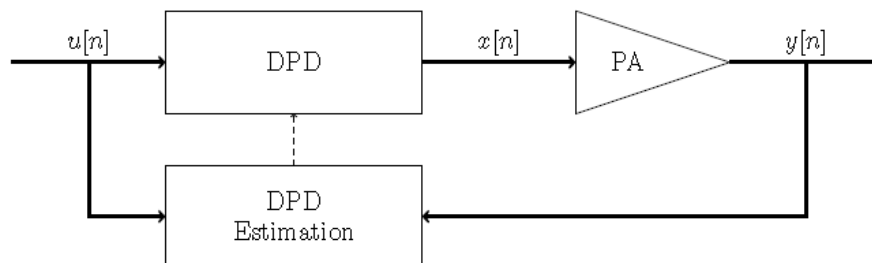


Figure 2.3 Indirect Learning Method

As depicted in Figure 2.3, the predistortion function can be defined as:

$$x[n] = u[n] - \mathbf{u}(n) \cdot \mathbf{w}(n)^T \quad (2-7)$$

where $u[n]$ is the original input signal and $\mathbf{u}(n)$ is a vector built from $u[n]$ according to the PA model. $\mathbf{w}(n)^T$ is the vector of DPD coefficients used to predistort the input signal. According to Theorem 1, if the vector of DPD coefficients is known and the nonlinear behavior of the PA remains time-invariant, the equation 2-10 is able to approach the inverse function of PA nonlinear behavior. Thus, the PA output signal will be the same as the original input signal times a linear gain.

The error between the original input signal and the PA output signal will be calculated in DPD estimation block, which is defined as

$$e[n] = y[n] - x[n] \quad (2-8)$$

Where $e[n]$ is the sequence of error between two signal. $y[n]$ and $x[n]$ are the sequences of PA output and original input signal, respectively.

When the error is obtained, the correction vector of DPD coefficients will be calculated through quadratic minimization algorithms,

$$\mathbf{U} \cdot d\mathbf{w} = \mathbf{e} \quad (2-9)$$

where \mathbf{U} is the DPD model matrix and $d\mathbf{w}$ is the correction vector.

The DPD coefficients will be updated by the correction vector to minimize the error. The equation of DPD coefficients updating is defined as follows,

$$\mathbf{w}(n + 1) = \mathbf{w}(n) + \lambda \cdot d\mathbf{w} \quad (2-10)$$

where n is the number of the adaptation iteration. The weighting factor λ is a value between 0 and 1 which can be either constant throughout all the adaptation or change at each iteration. Usually, the value of the weighting factor can be reduced at each iteration as the convergence of the method leads to a lower quantity of error and, therefore, a lower contribution from the new estimation [4].

It should also be noted that for the first adaptive iteration, the DPD coefficients $\mathbf{w}(0)$ is able to be initialized as $\vec{0}$.

2.2.2. Indirect Learning Method

The block diagram of the DPD extraction based in the indirect learning method is depicted in Figure 2.4.

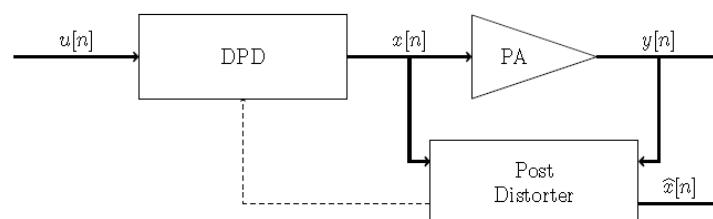


Figure 2.4 Indirect Learning Method

For indirect learning, which is depicted in Figure 2.4, the predistortion function is the same as the direct learning. The post-distortion part will simulate the procedure of DPD block according to the PA input and output signal, which is defined as:

$$\hat{x}[n] = y[n] - \mathbf{y}(n) \cdot \mathbf{w}(n)^T \quad (2-11)$$

where $y[n]$ is the PA output signal and $\hat{x}[n]$ is the estimated PA input signal, $\mathbf{y}(n)$ is the vector built from $y[n]$ according to the PA model and $\mathbf{w}(n)$ is also the DPD coefficients vector.

It is intuitive that the post-distortion part solves the inverse function directly use by inverting the input and output signal. When the variation happens on PA, the error will be calculated as:

$$e[n] = x[n] - \hat{x}[n] \quad (2-12)$$

where \vec{E} is the sequence of error between two signals. \vec{X} and $\vec{\hat{X}}$ are the sequence of PA input and estimated PA input signal, respectively.

The correction vector will be obtain as following by quadratic minimization algorithms:

$$\mathbf{U} \cdot d\mathbf{w} = e \quad (2-13)$$

where U_y is the DPD model matrix calculate by PA output signal according to the PA behavior model and $d\mathbf{w}$ is the correction vector.

Thus, the DPD coefficients will be updated as:

$$\mathbf{w}(n + 1) = \mathbf{w}(n) + \lambda \cdot d\mathbf{w} \quad (2-14)$$

where n is the number of the adaptation iteration. Similarly, for the first adaptive iteration, the DPD coefficients \vec{W}_0 is also able to be initialized as $\vec{0}$.

To summarize, both direct and indirect methods are suitable for applying the estimation of the DPD coefficients for the digital predistortion as the adaptive method. Although the indirect method looks intuitive, the direct method performs better under stringent ACLR requirements. In this thesis, all methods are based on direct learn method. The proofs of these two methods are in appendix I.

Since the feasibility of adaptive method is based on the linearity of the transformed PA responding function, to choose a suitable PA model to transform the PA responding function is critical in engineering application of DPD linearization. An inappropriate model may not only increasing the computational complexity and time consuming but it will also deteriorate the linearization performance. The effect of choosing the parameters of the Memory Polynomial model is depicted in Table 2-1. Alternating the coefficients will change the NMSE, that is, the difference between the real output and the model output and also the ACEPR, that is, how the spectrum of the model resembles the spectrum of the original output.

Polynomial Order	Memory Taps	Coefficients	NMSE [dB]	ACEPR [dB]	
				Lower	Upper
2	1	2	-20.4	-38.66	-38.31
2	7	14	-33.1	-39.15	-38.57
5	7	35	-40.1	-52.58	-52.08

Table 2-1 The DPD Performance in Different Parameters

2.3. The Feedback Path and the Importance of the Analog-to-Digital Converter (ADC)

As the name suggests, in comparison to the analog predistortion, the digital predistortion is performed in a digital signal processor at baseband. The DPD coefficients are extracted adaptively by comparing the input and output signal of PA. Since the PA output is in analog, it is pivotal to down-convert and digitize the PA output to compare with the original input signal. As a consequence the analog-to-digital converter (ADC) is a key element present in the DPD feedback loop.

To choose a suitable ADC in the DPD feedback loop is critical in the design of the DPD linearizer. Three major parameters should be taken into consideration. First, the resolution (number of bits) of the ADC, which means the numerical accuracy for representing the amplitude of the sampled analog signal. The second is the bandwidth, usually defined as Full Power Bandwidth (FPBW). This is the maximum allowed analog bandwidth supported by the ADC.. Finally, the most important parameter is the sampling frequency of ADC. It determines whether the analog signal will be properly digitized.

According to the classical sampling theory, the sampling frequency is defined to avoid the overlap distortion. The Shannon-Nyquist Theorem states that if a signal has no frequencies higher than B_0 hertz, then it will be completely represented by samples captured $1/(2B_0)$ seconds apart [14]. This theorem can be translated to a mathematical relation:

$$f_s \geq 2B_0$$

This relation means the sampling frequency f_s has to be, at least, two times larger than the highest frequency of the signal. Accordingly, the lowest sampling frequency is called the Nyquist frequency. This is the criterion for choosing the ADC in DPD linearizer, i.e. the sampling frequency of ADC has to be, at least, two times larger than the biggest valid frequency of the PA output signal. Therefore, taking into account current communication standards presenting high BW and high peak-to-average power ratios signals (such as the multi-carrier OFDM-based signals), the ADC sampling frequency has to be significantly high, which increases the cost and power consumption of the overall transmitter. With the same bandwidth and resolution, high frequency ADC is much expensive than lower ones, as depicted in Table 2-2.

Part #	Resolution	US Price 1000 to 4999	Sampling Rate	FPBW (typ)
AD9629-20	12	\$5.25	20 MSPS	700 MHz
AD9629-40	12	\$6.85	40 MSPS	700 MHz
AD9629-65	12	\$12.08	65 MSPS	700 MHz
AD9629-80	12	\$16.70	80 MSPS	700 MHz
AD9230-170	12	\$35.42	170 MSPS	700 MHz
AD9430-170	12	\$39.97	170 MSPS	700 MHz
AD9626-170	12	\$34.91	170 MSPS	700 MHz
AD9230-210	12	\$42.50	210 MSPS	700 MHz
AD9626-210	12	\$42.00	210 MSPS	700 MHz
AD9430-210	12	\$55.66	210 MSPS	700 MHz
AD9230-250	12	\$59.71	250 MSPS	700 MHz
AD9626-250	12	\$59.46	250 MSPS	700 MHz

Table 2-2 The Price of ADC with Different Frequency [15]

Therefore, the scope of this MSc. Thesis is studying the feasibility of operating the adaptive DPD linearizer with high under-sampling ratios. In this way, low frequency ADCs will be used to significantly decrease the cost and power consumption of the overall transmitter.

Chapter 3

Description of the Under Sampling Theory

3.1. Definition of Under Sampling

As discussed in section 2.3, the Shannon-Nyquist Theorem defines the minimum sampling frequency, called Nyquist frequency, for a given band-limited analog signal. For convenience, in this thesis, using the Nyquist frequency to sample an analog signal is called as the *full rate sampling* and the analog signal sampled in this way will be referred to *full rate sampled* signal. On the other hand, to use a frequency rate lower than the Nyquist frequency is called *under sampling* and also the analog signal is *under sampled*. The proportion between the actual sampling frequency and the Nyquist frequency is called the *under sampling ratio (USR)*, as defined:

$$USR = \frac{f_{sampling}}{f_{Nyquist}} \quad (3-1)$$

For instance, if a signal x presenting a bandwidth of 400 MHz is sampled at 800 MHz, which is exactly the Nyquist frequency, we will refer to full rate sampling. Instead, digitizing with a sampling rate of 100 MHz, means operating with an ADC with an under sampling ratio of 8.

3.2. DPD coefficients calculation

As discussed in section 2.2, the DPD coefficients are obtained adaptively using either the direct or indirect learning method. At each iteration, the DPD coefficients are updated by the correction vector, as shown in the following equation:

$$\mathbf{w}(n + 1) = \mathbf{w}(n) + \lambda \cdot \mathbf{dw} \quad (3-2)$$

Thus, the primary task for extracting the DPD coefficients is to obtain the correction vector. In direct learning method, the correction vector is calculated by the following equation:

$$\mathbf{X} \cdot \mathbf{dw} = \mathbf{e} \quad (3-3)$$

Also use the memory polynomial model as example, with an input digital sequence of L samples, the equation 3-3 will expands as:

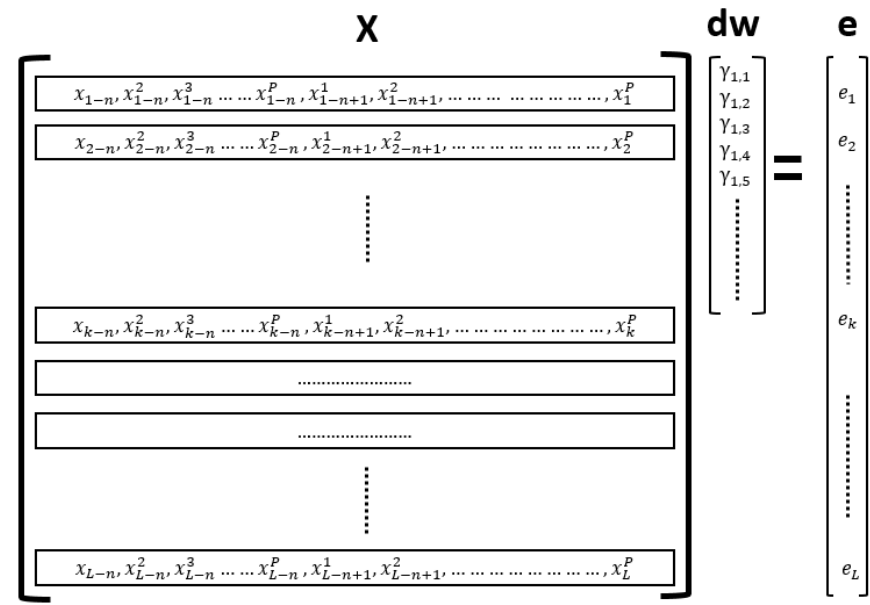


Figure 3.1 The Matrix of Memory Polynomial Model

The number of rows in the matrix is the same as the number of sample in the digital input signal, which is much more than the number of coefficients in DPD coefficients vector. The equation 3-3 is a linear regression model. In this thesis, it is called the DPD updating linear regression model (DULR). According to the Gauss-Markov theorem, the way to estimate the coefficients with least error is using the ordinary least squares methods. In this thesis, the recursive least squares method, one of the ordinary least squares methods, is used as a solver to this linear regression model, which is one of the ordinary least squares methods.

The objective of using the RLS method is to decrease the computational complexity and storage requirement of the DPD block. Unlike the least squares algorithms, the RLS divides the whole solving procedure into several parts and computes step by step. As shown in Figure 3.2, $X(i)$ is the sub-matrix of X , $e(i)$ is the sub-vector of e and the black columns are the row of matrix X in Figure 3.1.

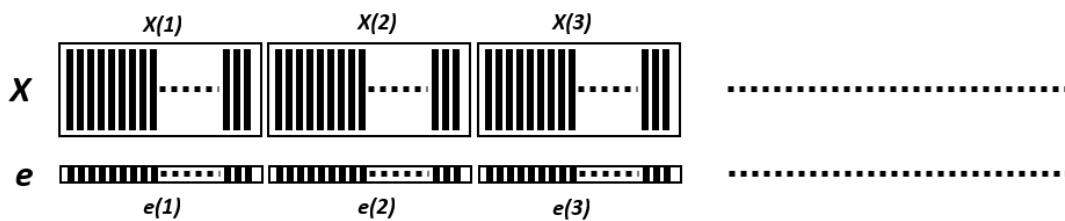


Figure 3.2 Matrix Division of the RLS Algorithm

For each step of iteration, the $\mathbf{w}(i)$ will be updated by $\mathbf{X}(i)$ and $\mathbf{e}(i)$. Following equations are used during the updating:

$$\mathbf{k}(n) = \frac{\lambda^{-1} \mathbf{P}(n-1) \mathbf{X}(n)}{\mathbf{1} + \lambda^{-1} \mathbf{X}(n)^T \mathbf{P}(n-1) \mathbf{X}(n)} \quad (3-4)$$

$$\boldsymbol{\alpha}(n) = \mathbf{e}(n) - \mathbf{X}(n)^T \mathbf{w}(n-1) \quad (3-5)$$

$$\mathbf{w}(n) = \mathbf{w}(n-1) - \mathbf{k}(n) \boldsymbol{\alpha}(n-1) \quad (3-6)$$

$$\mathbf{P}(n) = \lambda^{-1} \mathbf{P}(n-1) - \lambda^{-1} \mathbf{k}(n) \mathbf{X}(n)^T \mathbf{P}(n-1) \quad (3-7)$$

Where $\mathbf{k}(n)$ and $\mathbf{P}(n)$ are the Intermediate variables for iterating and λ is the forgetting factor of RLS. The initial value of \mathbf{P} is usually as $\mathbf{P} = \rho^* \mathbf{I}$, where \mathbf{I} is the unit matrix. Parameter λ and ρ are closely related to the converging and transit performance of RLS. In usual case of DPD implementation λ is typically smaller and close to 1, like 0.99 and 0.95, while ρ is 1.

3.3. The Statistical Sampling of the Linear Regression Model

In each iteration step of RLS method, the coefficient vector is corrected by:

$$\mathbf{w}(n) = \mathbf{w}(n-1) - \mathbf{k}(n) \boldsymbol{\alpha}(n-1)$$

As a recursive method, it is necessary to put a threshold to know when it will converge. The threshold of RLS is defined as:

$$\varepsilon_{\text{Residual}} = \frac{\text{mean}(\mathbf{k}(n) \boldsymbol{\alpha}(n-1))}{\text{mean}(\mathbf{w}(n-1))} \quad (3-8)$$

where $\text{mean}(\)$ stands for the *average value*.

The $\varepsilon_{\text{Residual}}$ is hereby used to evaluate the quantity of correction comparing with the coefficients vector. Normally, the RLS will converge after several iteration instead of completely calculating the whole matrix. Although the correction vector obtained from the RLS estimation will not be exactly the same as the one obtained from a normal least squares estimation, it will not affect the numerical accuracy of solving the linear regression problem [16].

The parts of the whole matrix that are used by RLS method is able to be considered as a statistical sample of the DULR, which means its linear regression coefficients of the DULR are able to be acquired from a given statistical sample. As this statistical sampling do not has any selectivity, it can be considered as an evidence for the statistical homogeneity of the DPD updating linear regression model. Thus, it remains the possibility of acquiring the coefficients from its other statistical sample.

On the other hand, let us consider the redundancy of each equation in the DULR. Similar as the linear equations, if two equations are high linearity dependent, they can be considered as one equation for linear solving. The linearity dependence is usually calculated by the Pearson product-moment correlation coefficient (PPMC). The PPMC is defined as:

$$\rho_{X,Y} = \frac{E(xy) - E(x)E(y)}{\sqrt{E(x^2) - E(x)^2} \sqrt{E(y^2) - E(y)^2}} \quad (3-9)$$

Where x , y are the two sequence of signal and $E()$ means the mathematical expectation of the sequence.

For simplicity, an example is shown in Figure 3.3.

$$\begin{cases} 2x + 3y = 10 & (1) \\ 4x + 6y = 20.001 & (2) \\ x + y = 17 & (3) \end{cases}$$

Figure 3.3 An Example of Linear Equation

The equation (1) and (2) are high linearity dependent (it equals to 1 in numerical calculation with dual-accuracy float data format), which means one of those equations is redundant in this linear equations. In other words, if a group of equations are highly linearity dependent, removing some of them will not affect the solution.

For the DULR, Figure 3.4 depicted the average PPMC value of nearby equations with a given gap. It is obvious that adjacent equations when considering low gap values have significantly high PPMC and by increasing the gap value, the average PPMC value decreases sharply. In this way, if we deleted the nearby equations that are closely linearity dependent, it will not only have no effect to the final solution of the linear regression but it will also diminish the number of redundant equation in the whole matrix.

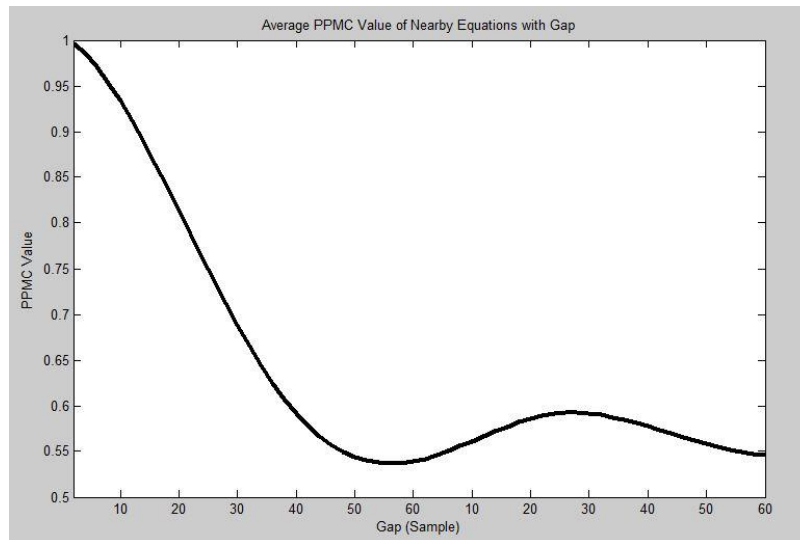


Figure 3.4 Average PPMC Value of Nearby Equations with a Given Gap

According to the statistical homogeneity and the trend of average PPMC value of nearby equations, a method for statistical sampling the DULR, called the Gap Sampling (GS), is proposed to extract the equations from DULR with a given gap, where the gap is called Statistical Sampling Gap (SSG). For instance, there are 100 equations in DULR which are numbered from 1 to 100 and the SSG is 2. The statistical sample will be a collection of the equations in DULR which has the odd index. It has a high possibility to characterize the statistic feature of the original DULR, i.e. to obtain the coefficient of the original DULR. If so, the DPD correction vector is able to be acquired from the GSS which has less equations and less equation redundancy.

In addition, the GS also offers a critical benefit when applying in DPD estimation. As discussed before, the error vector that is used to calculate the correction vector is defined in equation 2-11. In this equation, the input vector is already in digital format that can be used directly, but the output vector is digitized (using the ADC) with a given sampling frequency. When using GS, only a part of the samples in the output digital sequence are necessary for calculation, i.e. the part has gap between each other. This subsequence is easily to obtain by under sampling the analog output, which means that the ADC can work with a lower sampling frequency. In this way, low sampling frequency rate ADCs can be used in DPD feedback loop. As discussed in chapter I, this will significantly decrease the cost of DPD linearization design.

The DPD linearization using a low sampling frequency ADC will be referred from now on as Under Sampling DPD and the acronym will be US-DPD. The SSG will be the same as USR. Its DPD estimation part will also directly use the under sampled output sequence and its corresponding data matrix to calculate the DPD correction vector. As depicted in Figure 3.5, the equations that have the corresponding value in the output sequence will be extracted for calculating the DPD correction vector.

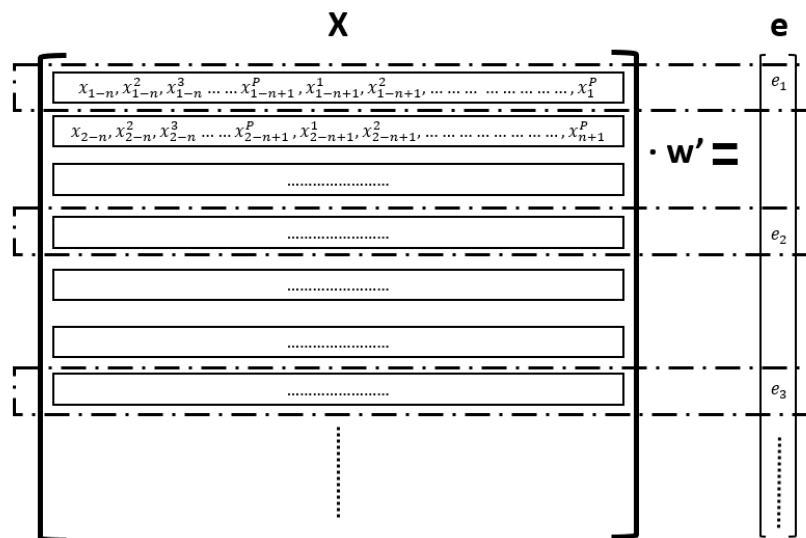


Figure 3.5 The Extraction of Equations in US-DPD

3.4. The Problem of Aliasing

According to the classical sampling theorem, if an analog signal is sampled at a low frequency below the Nyquist rate, then there will be aliasing or distortion due to the overlapping of the alias. Figure 3.6 shows the aliasing phenomenon.

Thus, following a traditional approach, in DPD linearization, the sampling frequency of ADC is always limited by this law, which means under sampling will lead overlap and cannot be used in DPD linearization. But it is worth noting that there is a fatal **definition interchanging** when using Shannon-Nyquist law in DPD linearization.

Figure 2.2 describes the differences between full rate sampling and under sampling. In stage I is the source signal, which is sampled by ADC and the restored by DAC into analog in stage II and stage III. The signal which passes through the under sampling ADC cannot be properly recovered because the sampling frequency is lower than required by Nyquist law, leading to alias overlapping. In contrast, in DPD linearization, the processing of signal remains in stage two, which means the signal will not be converted to analog format. In the digital domain, the only difference between under sampling and full rate sampling is that the former catches less samples while the VALUE of the caught samples are the same.

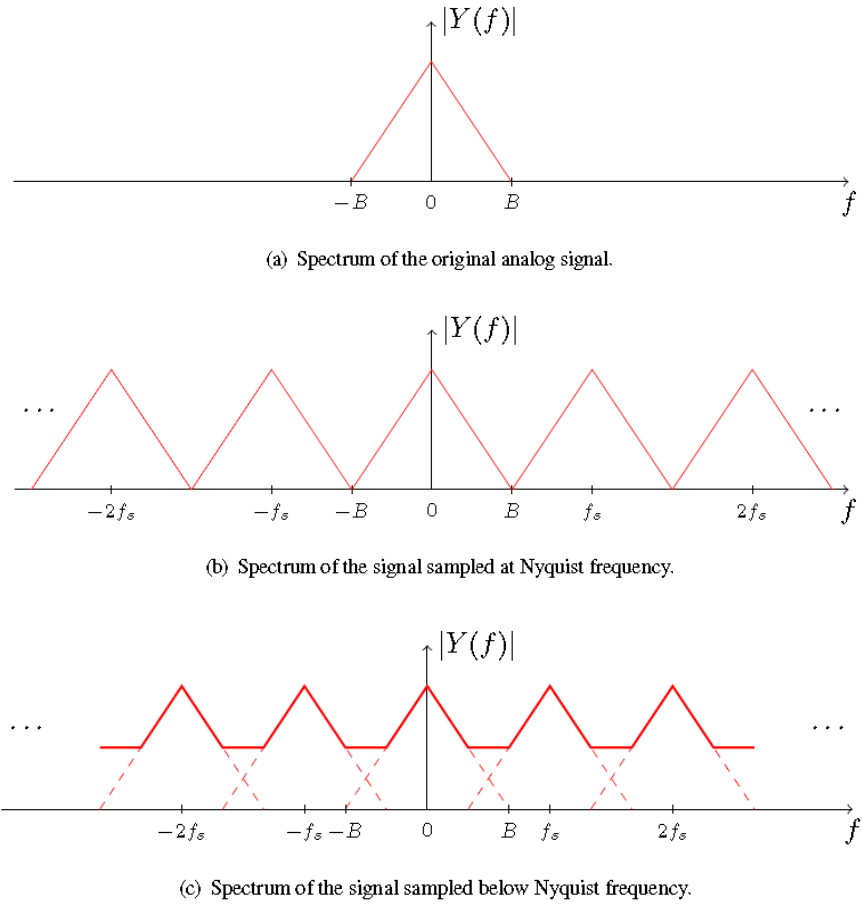


Figure 3.6 Effects of Aliasing when Sampling a Signal [1]

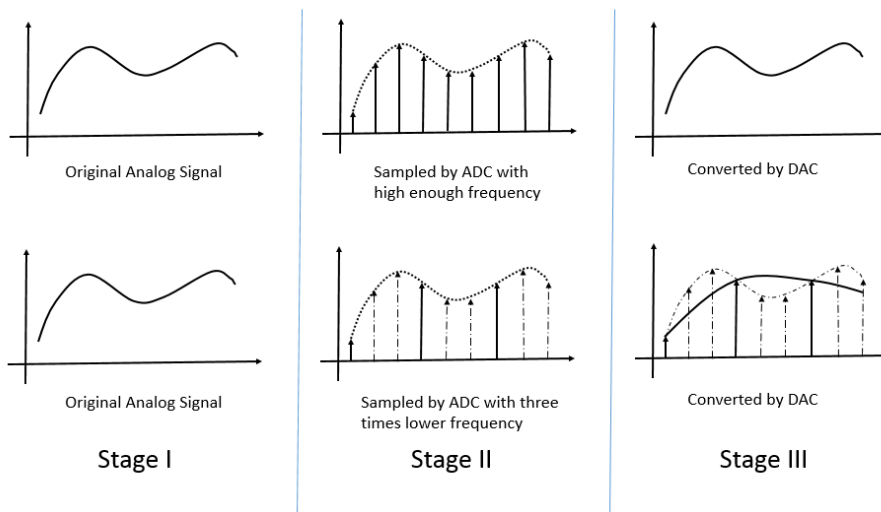


Figure 3.7 The Comparing of Full Rate Sampling and Under Sampling ADC-DAC Loop

This does not mean that the Shannon-Nyquist law is no longer valid in DPD linearization. The key point here is the definition interchanging. The conclusion of Shannon-Nyquist law is when the signal is sampled with a frequency lower than Nyquist frequency, it is impossible to recover the original analog signal, what happens in the third stage in Figure 3.7. But in all signal processing procedures of DPD linearization, as we have already discussed in this thesis, the requirement of *representing the input signal* has never appeared. The signal sample by ADC in DPD feedback loop will also never be converted to analog again in whole DPD process. The only thing that has a significant impact to DPD linearization in the feedback loop is the accuracy of ADC. This means that the digital value of the sequence sampled by the ADC should have enough accuracy to describe the actual value of the analog PA output signal at the sampling point, otherwise the DPD estimator will not be able to detect the behavior of DPD for predistortion. In this way, the *requirement* of sampling the analog signal in DPD linearization is not the same as what in Shannon-Nyquist law, which means Shannon-Nyquist sampling law is not related to the sampling procedure of DPD linearization.

This is the main principle of USR-DPD linearization. However, the under sampling frequency that can be used in the DPD identification also has its limitation, which will be discussed in next section.

3.5. Upper Limitation of the Under Sampling Ratio

Assuming that at the time of t_0 , the DPD linearization works ideally with a given PA, which means that the signal will be amplified pure linearly. In the next time period of t_{period} , the behavior of PA will change. This change is here by defined in broad sense, which includes the change of input signal feature, the thermal environment and so on. This specific change will only maintain in this time period and is able to be described as $\vec{\Delta\delta}$ of the DPD coefficient vector. Due to this change, the DPD linearizer needs to be updated to compensate the new PA behavior.

In practical way, this change of PA is usually evaluated by the NMSE of ACLR indicator. For example, the requirement of DPD linearizer performance is -25dB in NMSE, when the NMSE value increases over -25dB at a time, it means the PA behavior is changed.

In this way, the mission of DPD estimator is to detect the change and generate an accordingly correction vector to compensate this change and maintain the performance of DPD. As this specific change will only happen inside this time period, the correction vector will also only be valid inside this period. So, the DPD estimator is required to acquire this correction vector within $\frac{1}{k} t_{period}$, where k is a positive number, thus in the other $\frac{k-1}{k} t_{period}$ of time the signal will be amplified in a linear way. For simplicity, the time of calculation is not considered in this topic.

If the required number of equations of the DPD estimator to calculate the correction vector is already known as N_{USR} and not effected by the changing of PA behavior, the minimum required sampling frequency at the of ADC in DPD linearization, called as f_{USR} , can be calculated as:

$$f_{USR} = \frac{k \cdot N_{USR}}{t_{period}} \quad (3-10)$$

The N_{USR} is related to the linear regression solving method, complexity of PA model, the feature of input signal and so on. It is possible to approximate in experimentation.

In DPD linearization, the highest frequency of input signal is fixed and determined by the specific communication standard. The condition of using DPD linearization is limited as:

$$f_{USR} \leq f_{input} \quad (3-11)$$

Where f_{input} is the highest frequency of input signal.

Which means that the highest frequency of input signal is also limited the maximum number of equations in a given time. If the f_{input} is not enough large, the DPD linearizer will never have the sufficient equations to figure out the change of PA behavior.

Chapter 4

Aligning Problem

4.1. Problem Statement

In DPD calculation, the input and output signal are compared during calculating the DPD coefficients. As those two signals come from different path to DPD calculation part, there is a delay between two digital sequences that is caused by PA and other electronic component. Thus the input and output signal should be aligned first by detecting and fixing the delay. Normally, the cross-correlation function is used for this problem. The cross-correlation is a measure of similarity of two waveforms (two sequences if in discrete) as a function of a time-lag. For continuous functions f and g , the cross-correlation is defined as:

$$(f * g) (\tau) \stackrel{\text{def}}{=} \int_{-\infty}^{+\infty} f^*(t)g(t + \tau)dt \quad (4-1)$$

Where f^* denotes the complex conjugate of f and τ is the time lag.

For discrete functions, which is the signal sequence in this case, the cross-correlation is defined as:

$$(f * g) [n] \stackrel{\text{def}}{=} \sum_{m=-\infty}^{\infty} f^*[m] g[m + n] \quad (4-2)$$

Where f^* denotes the complex conjugate of f and m is the time lag as a unit of sample.

In DPD implementation, the value of cross-correlation of the input and output signal sequence will be calculated with a given range of possible delays. The delay with the highest cross-correlation value will be regarded as the delay between the two signals.

The condition for using the cross-correlation is that the both signal have to be digitized with the same sampling frequency [17]. In other words, the samples in these two sequence should match one by one. When implementing the under sampling, the output signal sequence has less samples than the input signal. In order to calculate the cross-correlation, the input signal will also be down sampled first. As shown in Figure 4.1, the values of cross-correlation are calculated by output signal and down sampled input signal with a given delay. Unfortunately, the delay with largest value is not the actual delay between the two sequences. Thus, it is not possible to use cross-correlation to detect the delay and align two sequences any more.

Input Signal	4	5	7	8	1	9	1	3	8	5	2
Output Signal	4		7		1		1				
Delay 0	4	5	7	8	1	9	1	3	8	5	2
<Actual delay>	4		7		1		1				
	$4*4 + 7*7 + 1*1 + 1*1$										= 67
Delay 1	4	5	7	8	1	9	1	3	8	5	2
		4		7		1		1			
	$4*5 + 7*8 + 1*9 + 1*3$										= 98
Delay 2	4	5	7	8	1	9	1	3	8	5	2
			4		7		1		1		
	$4*7 + 7*1 + 1*1 + 1*8$										= 44
Delay 3	4	5	7	8	1	9	1	3	8	5	2
				4		7		1		1	
	$4*8 + 7*9 + 1*3 + 1*5$										= 103

Figure 4.1 The Result of Cross-Correlation in Under Sampling Situation

4.2. Linearity Dependence Algorithm (LDA)

As discussed before, we cannot rely on the cross-correlation as a method to calculate the delay between the input and output signals in an under sampling DPD scenario. Thus, the new method under research should be able to evaluate the similarity between two sequences and not be influenced by the under sampling. The linearity dependence is the solution. Instead of the cross-correlation, the linearity dependence alignment (LDA) will calculate the Pearson product-moment correlation coefficient (PPMC) of the two signals.

As depicted in Figure 4.2, down sampling will not influence the linearity dependence between two sequences as long as the quantity of numbers is sufficient for numerical calculation. Similarly to the application of the cross-correlation method, the values of PPMC are also calculated with the output signal and the down sampled input signal. After calculating all the values in the possible range, the one with the highest PPMC is the actual delay between the two sequences.

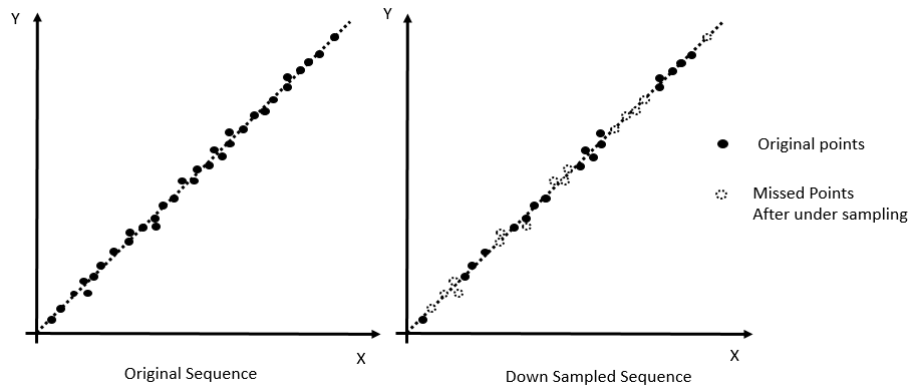


Figure 4.2 Linearity Dependence of Original Signal and Down Sampled Signal

Similar with application of cross-correlation function, the values of PPMC are also calculation by output signal and down sampled input signal with assumption delays. After calculated all the values in the possible range of actual delay, the assumption delay with the highest PPMC is the actual delay between the two sequences.

The LDA performance with under sampling is depicted in Figure 4.3. The sequence that has the delay will be down sampled first. The original sequence will be down sampled with a forced delay, as shown in Figure 4.2. The result of the forced delay detected by LDA is shown in 4.3, the green line is the actual delay value and the red dots are the delay value that detected by LDA. The result of LDA is remains stable while changing the USR.

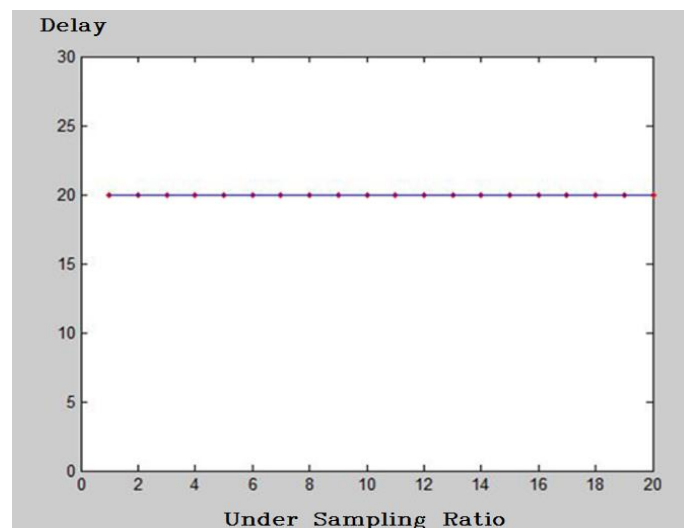


Figure 4.3 LDA Detection Result When Change USR

4.3. The Problem of Stability

On Figure 3.3 is the general calculation result of PPMC between two sequences with a delay. The assumed delay with highest PPMC value is chosen as the actual delay. It can be seen on Figure 3.3 that the difference between the values nearby the highest one is not significant. This phenomenon affects the numerical stability of LDA and increases the risk of having a wrong result. The influence of this risk will be discussed later in Chapter V.

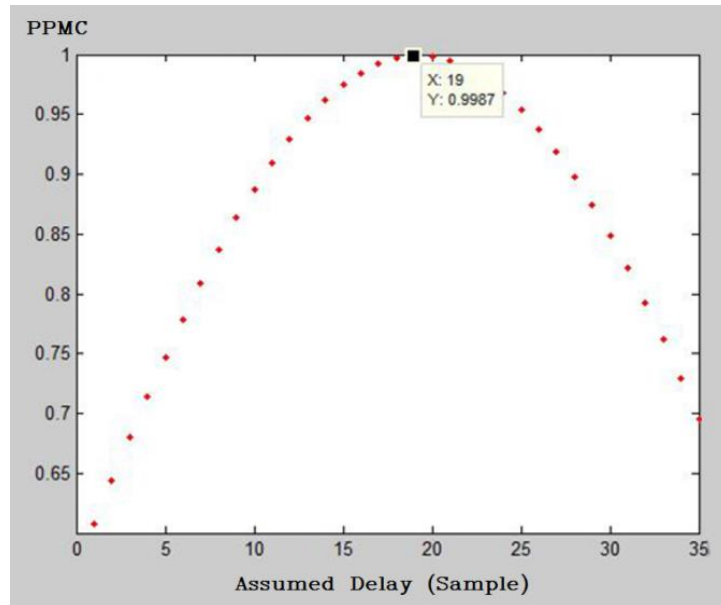


Figure 4.4 Linearity Dependence Value with different Delay Assumption

Chapter 5

Experimental Performance

The US-DPD and LDA methods that discussed in previous chapters will be tested using a real power amplifier. All the methods are coded in Matlab and connected to a test bench with a real device-under-test (DUT).

On the other hand, researchers also can do simulation test for DPD algorithms. In simulation, the PA behavior is simulated by the PA models, thus the PA behavior in simulation is limited due to the imperfection of PA models. However, despite the similarity of computational time consuming, the simulation test performance well in evaluating the capability of DPD algorithm itself. The simulation test is widely used in the primary experimentation of the DPD algorithm which will decrease the testing cost.

Comparing with numerical simulation, testing in a DUT needs lots of auxiliary facilities in addition to the DUT itself, which increases the complexity and also price. But testing with a real power amplifier and assembled instruments means the change of the signal between input and output is directly related to the power amplifying procedure, which mostly is the behavior of the PA. This allows researchers receive the first-hand experimental result of their theoretical contributions, which is helpful to improve the performance of design.

In this thesis, every testing case will be repeated for at least 3 times in case to have an averaging result.

5.1. Statement of Test Environment

5.1.1. Test Signal

Long term evolution (LTE) signal is chosen as the test signal for all the experimentations in this thesis. The LTE signal is based on OFDM with 20 MHz bandwidth. It is centered at DC frequency (the baseband), the spectral of LTE signal is depicted in Figure 5.1.

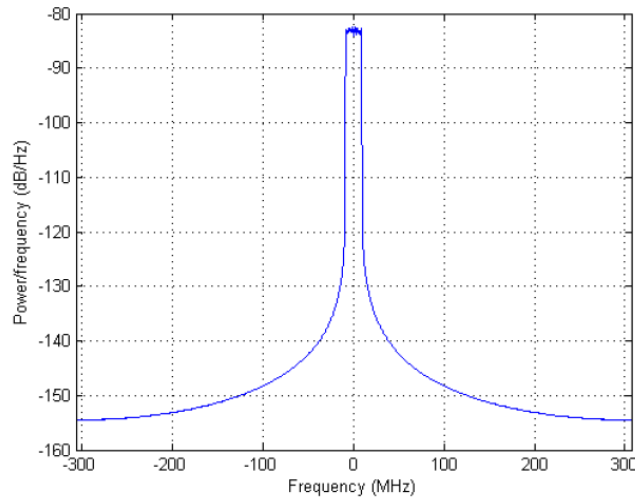


Figure 5.1 The Spectra of LTE Signal

5.1.2. Analog Amplifying Part

The analog amplifying part follows the schematic depicted in Figure 5.2. The digital signal is sent to the Texas Instruments TSW3084EVM Wideband Transmission Board which has an embed DAC34H84 Digital-to-Analogue Converter (DAC) and a TRF3705 I/Q Modulator, both also by Texas Instruments. The DAC has a resolution of 16-bit and a rate of 1250 MSa/s and the Modulator can output a signal up to 4 GHz in frequency. The Local Oscillator signal, which is sent to the Modulator as the carrier signal, is offered by an Agilent MXG Vector Signal Generator N5182A. In this thesis, the carrier signal is set to a frequency of 2 GHz and an amplitude of -10.0 dBm. In this step the complex digital signal will be converted to analog I-Q signal and then modulate to analog ratio-frequency signal with a carrier frequency of 2 GHz.

After being converted to analogue and modulated, the signal is sent through a Mini-Circuits pre-amplifier, model ZHL-4240 which provides a gain of +40 dB. The signal is then sent to the CREE CGH40006P Gallium- Nitride Power Amplifier capable of amplifying in frequencies up to 6 GHz and which is biased for AB-class operation.

In case to supply the power amplifier, an Arbitrary Waveform Generator is used as the supply of power amplifier. This Generator is able to amplify the input single properly, which is called the triggered model. In this way, the envelope signal that generated in Matlab based on the PA input signal, which is called *Env* in the diagram, is used to trigger the Arbitrary Waveform Generator to export the power supply signal of the PA according to the envelope signal, as discussed in Chapter I. On the other hand, when the Envelope signal is set as constant, the test environment then is in static supply.

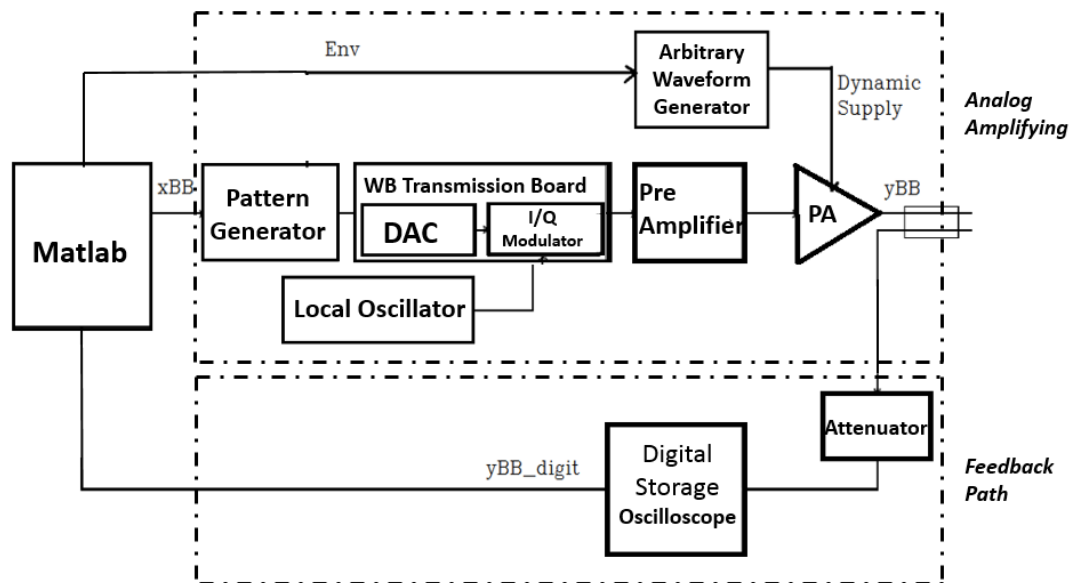


Figure 5.2 The Schematic of Experimentation Set-up

5.1.3. Feedback Path

Instead of real analog-to digital convertor (ADC), the digital storage oscilloscope is used in the feedback path of this experimental set-up. Although using the real ADC can strengthen the reality of this experimental, the parameter of the digital storage oscilloscope is able to be adjusted manually, which offers wider commissioning margin.

The feedback path starts with a Radiall R416020000 Attenuator which has a nominal attenuation of 20 dB. In order to reconvert the signal to digital samples for processing, an Agilent DSO90404A Oscilloscope is used, in which 2 GSa are obtained at a rate of 20 GSa/s.

5.1.4. Matlab Program and PA Model

In Figure 5.3 is the schematic of Matlab program. The test signal will first be generated in LTE format with 20 MHz bandwidth centered on baseband. The envelope of the test signal will be detected in Envelope Generator block and then sent to the Arbitrary Waveform Generator in the Analog Amplifying part. In case to compensate the behavior of PA while feeding dynamic supply, an two-demission DPD (2-D DPD) algorithm is applied [18]. The PA model used in 2-D DPD is defined as:

$$x[n] = \sum_{j=0}^M \sum_{q=0}^Q \sum_{i=0}^N \sum_{p=0}^P \gamma_{piqj} \cdot (E_s[n - \tau_j] - E_s^{Nom})^q \cdot u[n - \tau_i] \cdot |u[n - \tau_i]|^p \quad (5-1)$$

Where E_s is the envelope and u is the input signal. The γ_{piqj} are the DPD coefficients. M, Q are the memory depth and order for the envelope and N, P are the memory depth and order for the input signal. In this under sampling DPD test, the parameter of 2-D DPD is defined as: $M=3, Q=4, N=10, P=4$.

For direct learning, as discussed in Chapter II, the DPD coefficient matrix U will be the same for both DPD and DPD updating calculation. Thus, the matrix U will be first generated according to the test signal u and the envelope Env , as shown in Figure 5.3. In the DPD block, the distorted signal will be calculated according to the matrix U and the DPD coefficients vector following the equations of direct learning method.

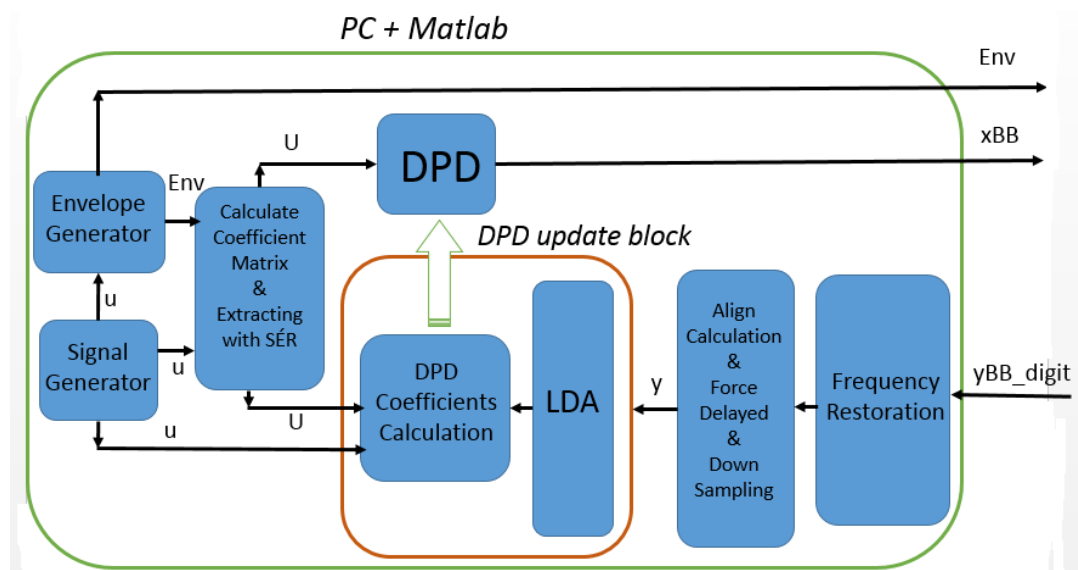


Figure 5.3 The Diagram of Matlab Program

For observation, the digital signal sampled by Digital Storage Oscilloscope, which is called y_{BB_digit} in the diagram, will be restored to a complex digital sequence with a sampling rate of 61.44 MSa/s in the block of *Frequency Restoration*, which is the same frequency as the test signal u . In case to observe the whole distortion behavior of PA in adjacent channels, the bandwidth of the output signal will be 100 MHz, i.e. five time the bandwidth of input signal as discussed in Chapter I. After that, the output signal will be aligned with the input signal using the traditional cross-correlation method and then be forced delayed with a given delay value. Using this aligning-delaying method, the delay value of the input and output signal will be a known value and it is possible to use those two signal to test the feasibility of the LDA.

The output signal with forced delay will be down sample with a given USR. In this way, the output signal y in the diagram will be the same as the output single of a real ADC with the same sampling frequency, and thus the feedback loop with an ADC is now simulated.

In DPD update block, the LDA will firstly detect the forced delay between input signal and down sampled output signal and then align them. The error of those signals will

also be calculated latter aligned. The extracted DPD coefficients Matrix and the error will be used to figure out the DPD correction vector as discussed before.

In this thesis, RLS method is coded in DPD Coefficients Calculation block to evaluate the relative time and equations quantity requirement of DPD algorithm. The iterating of RLS method will stop when $\varepsilon_{\text{Residual}}$ (the residual of RLS method which is defined in equation 3-8) is lower than the preset threshold. When the DPD parameter, i.e. the depth and order, is the same, for each iteration of RLS the number of equations will also be the same. Thus, the total iteration number of RLS with same $\varepsilon_{\text{Residual}}$ before DPD achieve the performance threshold can reflect the required quantity of equations and also the consuming of calculation. The DPD performance threshold is usually set as the value of NMSE or ACLR as discussed before. For all experimentations, the threshold of RLS $\varepsilon_{\text{Residual}}$ is set as 5%.

5.2. LDA Instability Evaluation

As discussed in Chapter IV, the difference between the maximum and nearby values is not significant. This leads to a possibility of producing a small quantity deviation of LDA result. A further test is implemented to evaluate the effect of this possible deviation to the DPD performance.

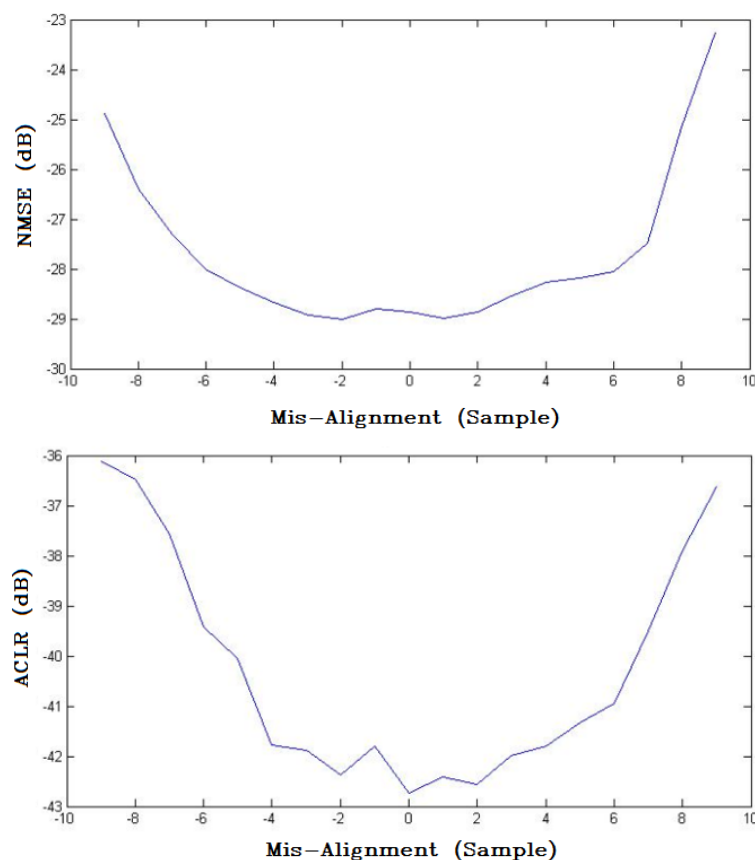


Figure 5.4 NMSE and ACLR Values When Misalignment Happens on DPD

The DPD performance influenced by misalignment is depicted on Figure 5.3. Normalized Mean Square Error (NMSE) and Adjacent Channel Leakage Ratio (ACLR) are used to evaluate the performance of DPD linearization. It is shown that the deterioration increases significantly with the growth of mis-alignment value. Besides, the absolute value of misalignment do not significantly affect the DPD result when it is very small. In this case, when the value of mis-alignment is lower than 3, the performance of DPD reminds the same level. The maximum absolute value that does not affect the DPD performance will be defined as the *DPD linearization Tolerance Radius* for the mis-alignment.

Given the tolerance radius of DPD linearization, the deviation of LDA results (assuming it happens) will only influent the LDA result itself but will not deteriorate the DPD performance. The testing of LDA is also implemented on the same test schematic above. The DPD performance with LDA is stated on Figure 5.5 . LDA algorithm detects the forced misalignment and maintains the performance of DPD.

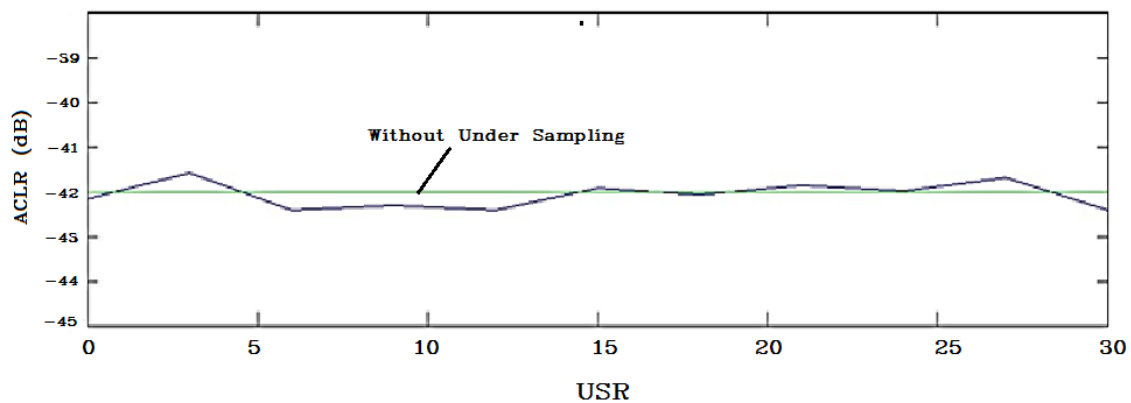


Figure 5.5 The DPD performance in ACLR with Forced Delay and LDA Restoration

5.3. Experimental Result of US-DPD

On Figure 5.6 are the numbers of RLS iterations that DPD linearization needs to achieve the given performance. In this case, the performance requirement is evaluated by ACLR and NMSE values. According to Figure 5.5, the number of iterations decreases while USR is rising. In the period of low USR, the more accurate the DPD threshold is, the drop of iteration number is more significant. When USR becomes larger, the number of iteration remains stable.

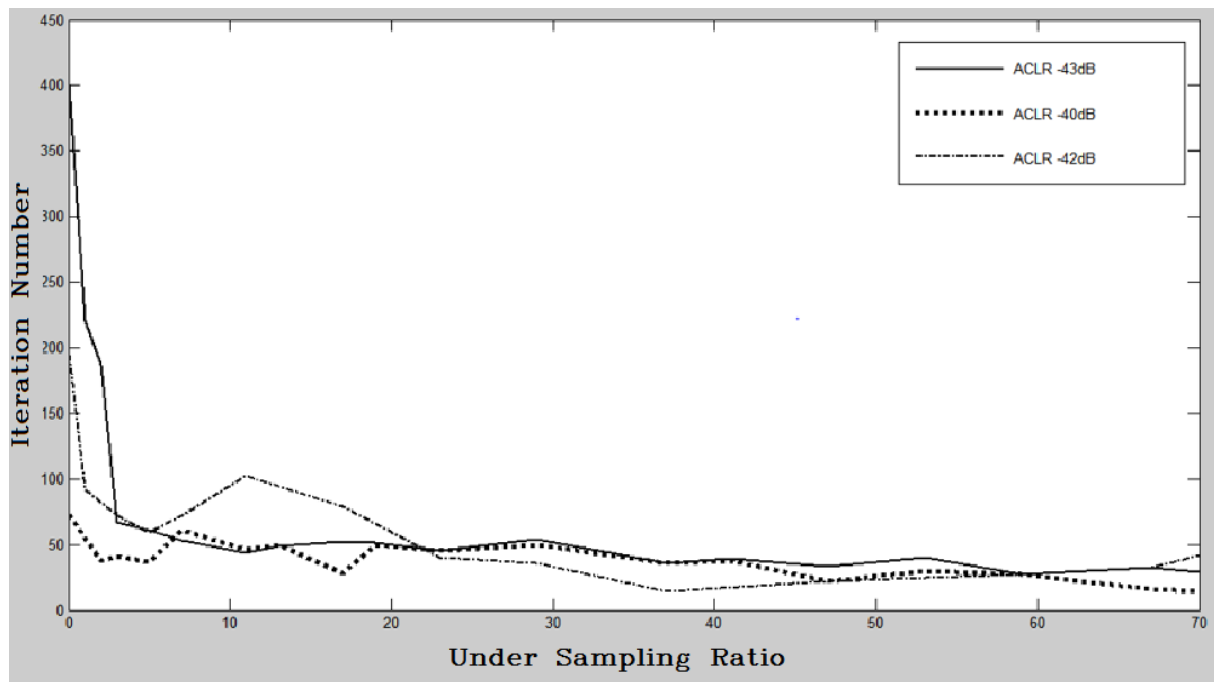


Figure 5.6 Iteration numbers in Different USR and Different DPD Threshold, Static Supply

The DPD performance when applying dynamic supply is depicted in Figure 5.6. Similarly as using static supply, under sampling decreases the computational demanding for DPD linearization.

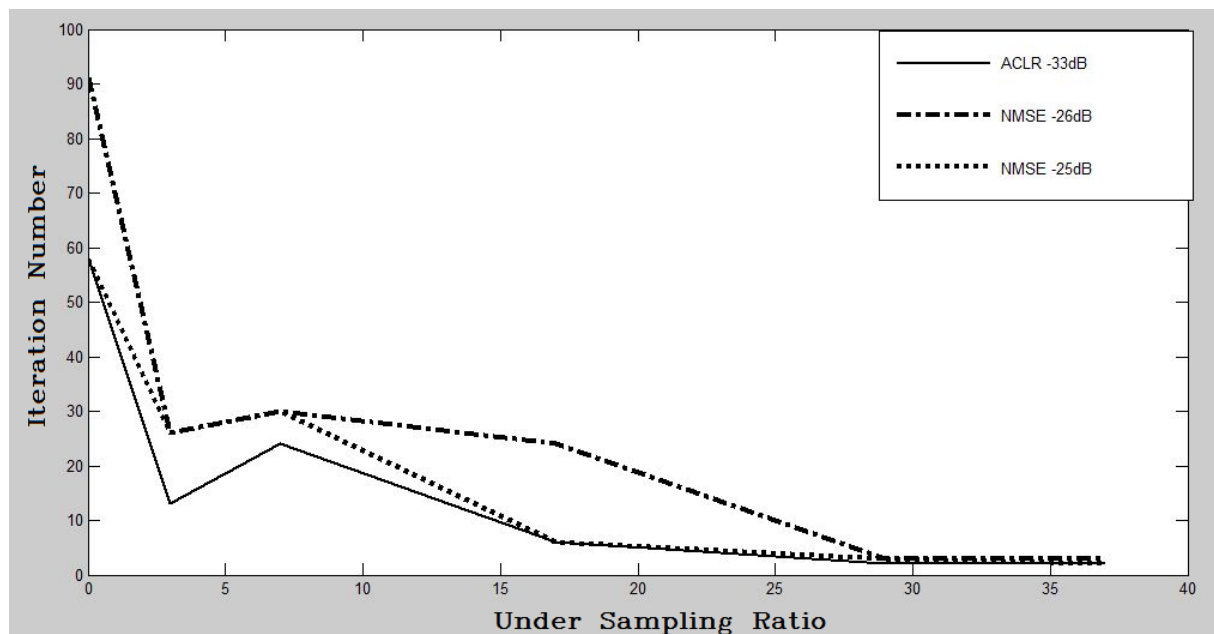


Figure 5.7 Iteration Numbers in Different USR and Different DPD Threshold, Dynamic Supply

In addition, DPD linearization is able to compensate the *spectral regrow* in different USR, as depicted in Figure 5.7. Besides, the distortion of signal, which is evaluated by NMSE, also has no significant fluctuation.

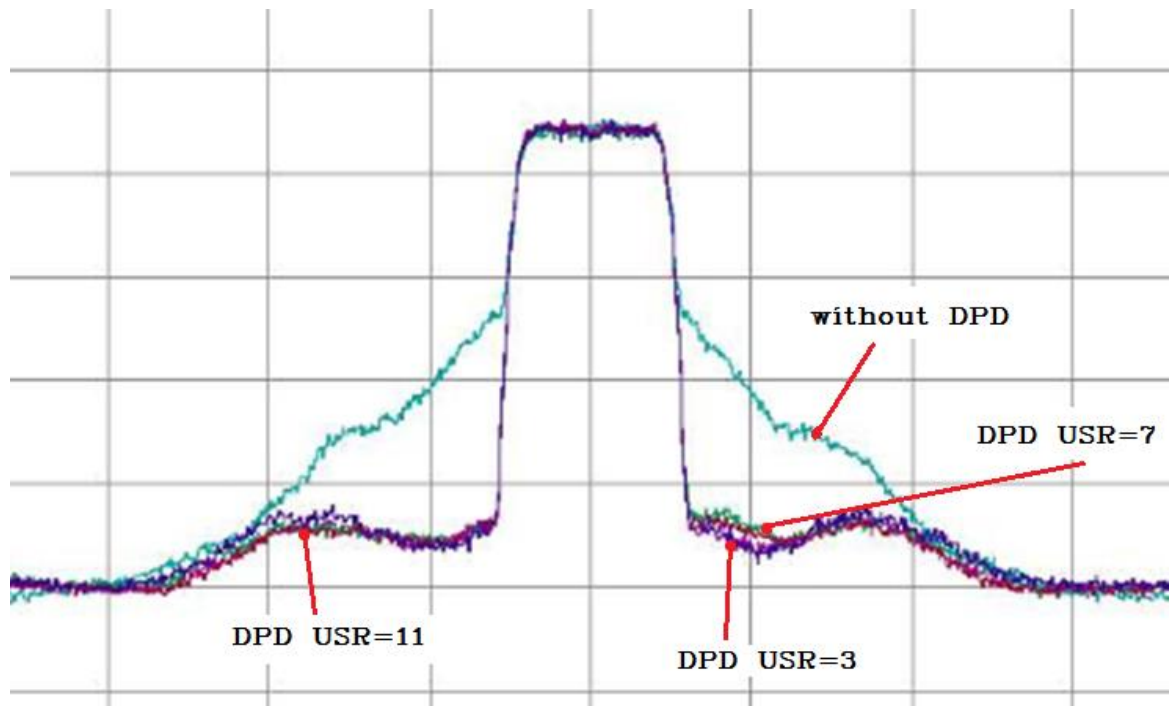


Figure 5.8 DPD Performance in Different USR

USR	NMSE (dB)
0	-27.3826
3	-27.7907
7	-27.6377
17	-26.3427
29	-27.6827
37	-27.0021

Table 5-1 DPD Performance Evaluated by NMSE in Different USR

Chapter 6

Conclusions

Applying US-DPD can significantly reduce the requirement of ADC sampling frequency without influencing the performance of DPD linearization. At the same time, US-DPD decreases the redundancy of the Matrix, which reduces the time consuming and computational consumption of DPD algorithm for reaching the acceptable performance. The limitation of ADC sampling frequency is regulated as following:

$$f_{ADC} \geq \frac{k \cdot N_{US}}{t_{period}} \quad (6-1)$$

Correspondingly, linearity dependence alignment (LDA) based on Pearson product-moment correlation coefficient (PPMC) is able to detect the delay of feedback loop in under sampling situation to align the input and under sampled output signal when traditional aligning methods do not work.

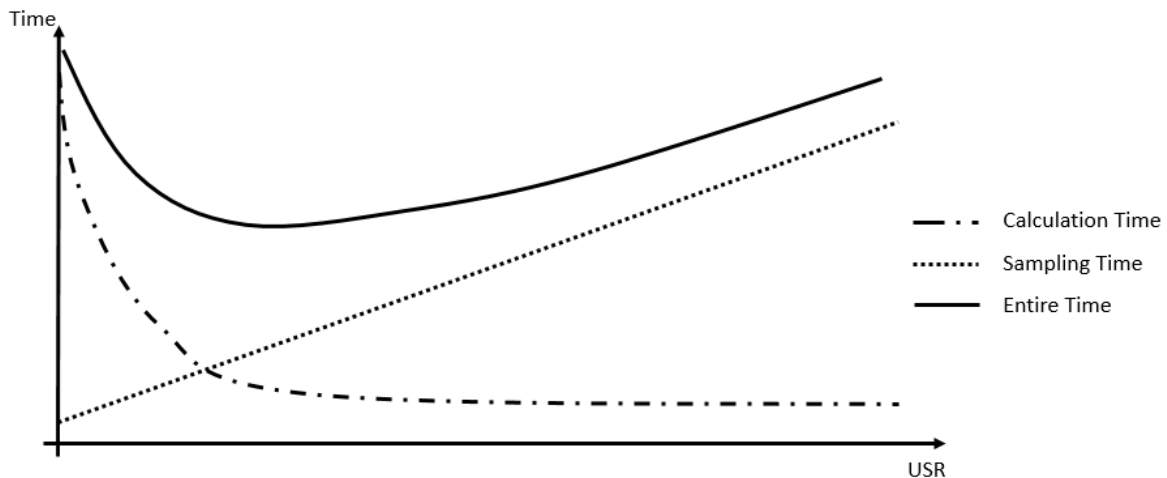


Figure 6.1 Entirety Time of DPD Updating with USR

Another aspect of US-DPD is the ENTIRE time consuming of DPD updating procedure. Although the time of calculation will decrease as discussed before, it takes more time to collect sufficient samples as the sampling frequency (i.e. the number of samples it takes per second) is reducing by USR. Thus, as shown in Figure 6.1, the entire time consuming equals to the sampling time plus the calculation time. In the view of time efficiency, engineers need to consider the compromising between them.

Bibliography

- [1]: Alibaba.com
- [2]: RCUnivers.com
- [3]: Futaba.com
- [4]: Pedro Sousa, Digital "Predistortion of Wideband Satellite Communication Signals with Reduced Observational Bandwidth and Reduced Model Order Complexity", Instituto Superior Tecnico, Lisbon, Portugal, Nov, 2014
- [5]: Yang Li ; Zhu, R. ; Prikhodko, D. ; Tkachenko, Y. "LTE power amplifier module design: Challenges and trends", Solid-State and Integrated Circuit Technology (ICSICT), 2010 10th IEEE International Conference on DOI: 10.1109/ICSICT.2010.5667803 Publication Year: 2010 , Page(s): 192- 195
- [6]: Pedro Pablo Vizarreta Paz, "Design and Implementation of an Envelope Tracking Power Amplifier Using Switched Amplifiers and Slow Envelopes", Universitat Politecnica de Catalunya, July 2011
- [7]: Gilabert, P.L.; Montoro, G. "Design and Implementation of an Envelope Tracking Power Amplifier Using Switched Amplifiers and Slow Envelopes Look-Up Table Implementation of a Slow Envelope Dependent Digital Predistorter for Envelope Tracking Power Amplifiers", Microwave and Wireless Components Letters, IEEE Volume:22, Issue: 2, Page(s): 97- 99, 2012
- [8]: A. Soto, J. Oliver, J. Cobos, J. Cezon, and F. Arevalo, "Power supply for a radio transmitter with modulated supply voltage," in Applied Power Electronics Conference and Exposition, 2004. APEC '04. Nineteenth Annual IEEE, vol. 1, 2004, pp. 392-398 Vol.1.
- [9]: José Carlos Pedro and Nuno Borges Carvalho. Intermodulation Distortion in Microwave and Wireless Circuits. Artech House, 2003. ISBN: 1580533566.
- [10]: R. Neil Braithwaite. Model order selection for digital predistortion of a RF power amplifier when the distortion spectrum exceeds the observation bandwidth. International Journal of Microwave and Wireless Technologies, 5:163–170, April 2013. ISSN 1759-0795. DOI: 10.1017/S1759078713000020
- [11]: Joel Vuolevi and Timo Rahkonen. Distortion in RF Power Amplifiers. Artech House, 2003. ISBN: 1580535399.
- [12]: A. Ahmed, S. M. Endalkachew, and G. Kompa. Power amplifier linearization using memory polynomial predistorter with non-uniform delay taps. In Microwave Symposium Digest, 2004 IEEE MTT-S International, volume 3, pages 1871–1874, June 2004. Doi: 10.1109/MWSYM.2004.1338972.
- [13]: R. Neil Braithwaite. Principles and Design of Digital Predistortion. In Fa-Long Luo, editor, Digital Front-End in Wireless Communications and Broadcasting —

Circuits and Signal Processing, chapter 6. Cambridge University Press, 2011. ISBN: 9781107002135.

- [14] : C.E. Shannon. Communication in the presence of noise. Proceedings of the IEEE, 86[2]:447–457, Feb 1998. ISSN 0018-9219.
- [15] : Analog.com
- [16] : Alexander, S. T.; Pan, C. T.; Plemmons, R. J., “Analysis of a Recursive Least Squares Hyperbolic Rotation Algorithm for Signal Processing”, LINEAR ALGEBRA AND ITS APPLICATIONS 98:3-40, 1988
- [17] : Braithwaite, R.N. "Wide bandwidth adaptive digital predistortion of power amplifiers using reduced order memory correction", Microwave Symposium Digest, 2008 IEEE MTT-S International, Page(s): 1517-1520, 2008
- [18] : Gilabert, P.L.; Montoro, G., “Look-Up Table Implementation of a Slow Envelope Dependent Digital Predistorter for Envelope Tracking Power Amplifiers”, Microwave and Wireless Components Letters, IEEE Volume:22, Issue: 2 Page(s): 97- 99, 2012